Quantitative Engineering Systems Modeling and Analysis of the Energy-Water Nexus

William N. Lubega, Amro M. Farid

Abstract

The *energy-water nexus* has been studied predominantly through discussions of policy options supported by data surveys and technology considerations. At a technology level, there have been attempts to optimize coupling points between the electricity and water systems to reduce the water-intensity of technologies in the former and the energy-intensity of technologies in the latter. To our knowledge, there has been little discussion of the energy-water nexus from an engineering systems perspective. A previous work presented a reference architecture of the energy-water nexus in the electricity supply, engineered water supply and wastewater management systems developed using the Systems Modeling Language (SysML). In this work, bond graphs are used to develop models that characterize the salient transmissions of matter and energy in and between the electricity, water and wastewater systems as identified in the reference architecture. These models, when combined, make it possible to relate a region's energy and municipal water consumption to the required water withdrawals in an input-output model.

NOMENCLATURE

$\boldsymbol{\Delta T_W}$	Permissible temperature increases of water sources
$\boldsymbol{\Gamma_G}$	Induced photocurrents at locations of solar photovoltaic installations
$\boldsymbol{\lambda_G}$	Wind speed at locations of wind farms
$\mathcal{H}_{\boldsymbol{G}}^{\boldsymbol{flue}}$	Specific sensible heat content of generator flue gas
$\mathcal{H}_{\boldsymbol{G}}$	Lower heating value of fuel used at generators
$\boldsymbol{\pi_W}$	Osmotic pressure of water sources
$\dot{\mathfrak{M}}_{\mathbf{G}}$	Process steam flow rate in thermal generators
$\dot{\mathbf{M}}_{\mathbf{G}}$	Fuel consumption of generators
$\mathbf{I}_{\mathcal{P}}$	RMS Current drawn by pumps in water distribution network
$\mathbf{I_D}$	RMS Current drawn by wastewater treatment facilities
$\mathbf{I_F}$	RMS Current drawn by water treatment plants
$\mathbf{I_G}$	RMS Current supplied by generators
$\mathbf{I_L}$	RMS Current drawn by all electrical load nodes
$\mathbf{I_N}$	RMS Current drawn by pipes and pumps in non-potable recycled wastewater distribution network
$\mathbf{I_{L_o}}$	RMS Current drawn by all electrical nodes excluding current for water system purposes
$\mathbf{P_D}$	Pressures imposed by wastewater treatment plants on non-potable recycled wastewater distribution network
$\mathbf{P_F}$	Pressures imposed by water treatment plants on water distribution network
$\mathbf{P_J}$	Pressures at non-potable recycled wastewater demand nodes
$\mathbf{P_J}$	Pressures at water demand nodes
$\mathbf{P_W}$	Pressures of water sources
$\mathbf{Q}_{\mathcal{P}}$	Water flow rate through pipes
$\mathbf{Q_D}$	Throughput of wastewater treatment facilities
$\mathbf{Q_D}^{disp}$	Disposable effluent production rate at wastewater treatment facilities

William N. Lubega is with the Engineering Systems and Management, Masdar Institute of Science and Technology, Abu Dhabi,UAE. wlubega@masdar.ac.ae

Amro M. Farid is an Assistant Professor with the Engineering Systems & Management Department of the Masdar Institute of Science and Technology. He is also a Research Affiliate with the MIT Mechanical Engineering Department.afarid@masdar.ac.ae, amfarid@mit.edu

$\mathbf{Q_D}^{rec}$	Non-potable recycled wastewater production rate at wastewater treatment facilities
$\mathbf{Q_E}$	Water demand rate at non-potable recycled wastewater demand nodes
$\mathbf{Q_F}$	Water supplied by water treatment and desalination plants
$\mathbf{Q_F}^{brine}$	Brine produced by water treatment and desalination plants
$\mathbf{Q_G}^{evap}$	Water evaporation rate associated with electrical generation units
$\mathbf{Q_G}^{in}$	Water withdrawal rate by generators
$\mathbf{Q_G}^{out}$	Generator effluent flow rate
$\mathbf{Q_J}$	Water demand rate at demand nodes
$\mathbf{Q_S}$	Water withdrawal rate from water storage units
$\mathbf{Q_S}^{evap}$	Water evaporation rate from water storage units
$\mathbf{Q_W}$	Water withdrawal rate from sources
$\mathbf{Q_{El}}$	Water leakage rate at non-potable recycled wastewater demand nodes
$\mathbf{Q_{Jl}}$	Water leakage rate at demand nodes
$\mathbf{V}_{\mathcal{P}}$	RMS Voltages applied to pumps in water distribution network
$\mathbf{V_F}$	RMS Voltages applied to water treatment plants
$\mathbf{V_G}$	RMS Voltage at generators
$\mathbf{V_L}$	RMS Voltage at electrical loads
$\mathbf{V_N}$	RMS Voltages applied to pumps in non-potable recycled wastewater distribution network
p_{atm}	Atmospheric pressure

I. Introduction

A. Motivation

The energy-water nexus can be defined [1]–[4] as a system-of-systems composed of one infrastructure system with the artifacts necessary to describe a full energy value chain and another infrastructure system with the artifacts necessary to describe a full water value chain. Large volumes of water are withdrawn and consumed from water sources every day for electricity generation processes [5]. Simultaneously, extraction, treatment and conveyance of municipal water and treatment of wastewater are dependent on significant amounts of electrical energy [5].

This *energy-water nexus*, which couples the critical systems upon which human civilization depends, has long existed but is becoming increasingly strained due to a number of global mega-trends [6]: (i) growth in total demand for both electricity and water driven by population growth (ii) growth in per capita demand for both electricity and water driven by economic growth (iii) distortion of availability of fresh water due to climate change (iv) multiple drivers for more electricity-intensive water and more water-intensive electricity such as enhanced water treatment standards,water consuming flue gas management processes at thermal power plants and aging infrastructure which incurs greater losses.

B. Literature Gap

A number of discussions on the energy-water nexus have been published in recent years. Overviews of the various challenges related to the nexus, as well as discussions of various policy options for the amelioration of the risks can be found in [6]–[12]. Empirical evaluations of the electricity-intensity of water technologies and the water-intensity of electricity technologies have been reported and analysed in [13]–[18]. Efforts have been made towards physics-based models in [19], [20] in which formulations for estimating water use by thermal power plants based on the heat balance of the plant have been derived. An integrated operational view of the water and power networks has also been presented as a simultaneous co-optimization for the economic dispatch of power and water [21]–[27].

Less literature is available on the development of tools for integrated management of electricity and water supply systems. A decision support system for the United States based on an underlying system dynamics model is described in [28]. The model enables the exploration of various water and electricity policies and relies on statistical relationships between the independent variables of population and economic growth and the dependent variables of electricity and water demand. Recent work [29] has interfaced the well known Regional Energy Deployment System

(ReEDS) and Water Evaluation and Planning (WEAP) tools to create a platform for determining the water resource implications of different electricity sector development pathways. The platform uses empirical consumption and withdrawal coefficients reported in [16] for the interface.

To the authors' knowledge however, a transparent physics-based model that interfaces a model of the electricity system to models of the municipal water and wastewater systems enabling an input-output analysis of these three systems in unison has not been presented. This work attempts to present and apply this *system-of-systems* model.

C. Scope

This paper adopts, as it's modeling scope, the engineered electricity, water and wastewater infrastructure as well as critical energy and matter flows across a system-of-systems boundary encompassing these three interconnected systems.

D. Relevance

The holistic, integrated modelling approach presented in this paper is of particular relevance to places with integrated electricity and water utilities (e.g. countries in the Gulf Cooperative Council (GCC)). The model enables the evaluation and comparison of different technology levers across the three systems of interest thus informing management and government policy around water, environment and energy. The modeling approach may also be applied to regions with separate electricity, water and wastewater utilities to demonstrate potential areas of coordination.

E. Contribution

In this paper, a quantitative, physics-based, engineering systems model of the energy-water nexus is developed as a first of its kind. This is in contrast to the existing literature which either has a smaller scope or uses empirical evaluations of water and energy intensity. The model uses *first-pass* but *often-cited* engineering models of various exchanges of matter and energy in and between the electricity, water and wastewater systems. Hence, the paper has a foundational nature in two regards. The *first-pass* engineering models replace the various empirical data surveys on the water intensity of energy technologies and energy intensity of water technologies [13], [15]. Also, the first-pass models may be refined in the future as per the needs of the analytical application. The presented model builds upon a reference architecture previously provided in [2] and is thus a reference model that can: (i) provide a foundation for qualitative discussions in the general case, and (ii) be instantiated for quantitative analysis of a particular case as in Section VII .

F. Paper Outline

The remainder of this paper continues in four sections. The bulk of the paper is devoted to the development and presentation of models. This is achieved sequentially. First, a high level systems-of-system view is given in Section II. Then each of three component infrastructure systems: electricity, water, and wastewater are addressed in Sections III, IV and V respectively. Section VI gives a recapitulation of the model in terms model outputs of interest. Section VII then presents an illustrative example in which the developed models are used to analyze the exchanges of energy and water in a simple, hypothetical geographical region. Finally, Section VIII concludes.

II. Systems-of-Systems Modeling

This section delineates the system boundary and proceeds to describe the modeling strategy that is employed for the following three modeling sections.

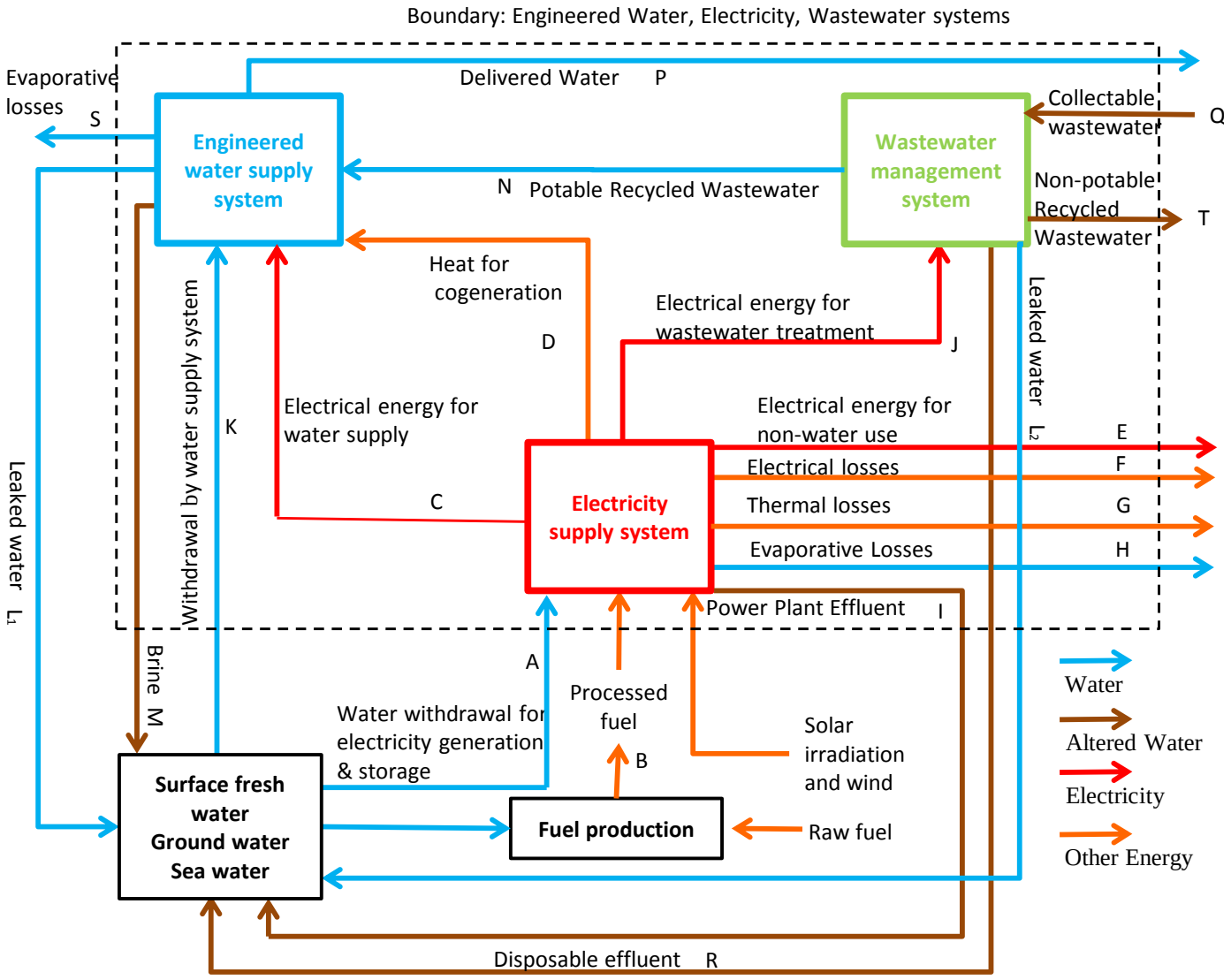

Fig. 1. System Context Diagram for Combined Electricity, Water & Wastewater Systems

A. System Boundary and Context

Figure 1 chooses the system boundary around the three engineering systems of electricity, water and wastewater [1]–[4]. It also depicts the high level flows of matter and energy between them and the natural environment. The labels A through S represent key flows of interest across the system boundary and between the three infrastructure systems. A subset of these are determined for the illustrative example in Section VII and used to determine certain measures of interest.

Electricity, potable water, and wastewater are all primarily stationary within a region's infrastructure. In contrast, the traditional fuels of natural gas, oil, and coal are open to trade. Consequently, the fuel processing function, though it has a significant water footprint, is left outside of the system boundary. An advantage of this choice of system boundary is that the three engineering systems all fall under the purview of grid operators; and in some nations, such as the United Arab Emirates, all three grid operations are united within a single semi-private organization. The system context diagram shown in Figure 1 makes it possible to relate a region's energy and municipal water use to the required water and energy withdrawals in a complex input-output model.

B. Modeling Strategy

The model presented here is built upon the foundation of a previously developed graphical model described in SysML [1]–[4]. This model showed that the energy-water nexus is not just composed of many component artifacts

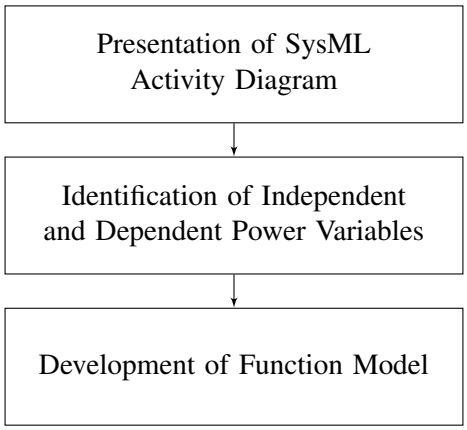

Fig. 2. Modeling Strategy

but also a large heterogeneity of functions; each with multiple input and output flows of matter and energy. The model presented here is the quantification of the previous work and thus develops a set of equations for each function found within the energy-water nexus. While the number of equations and variables for each function is modest, the shear heterogeneity of functions within the energy-water nexus necessitates that the full model be quite large to cover the full scope of interest.

The modeling strategy for this work progresses in three steps as shown in Figure 2. The system context diagram shown above allows for the mathematical modeling of each of the individual infrastructure systems and their respective components. Each infrastructure system is taken in turn using the same modeling strategy. First, a SysML activity diagram [30] is presented for the full scope of the engineered infrastructure system of concern. This allows for activity blocks to be defined for each of the component functions within the engineered system. Second, in order to transition from the graphical SysML language to a mathematical model each input and output associated with an activity block is represented as a flow of power in its respective energy domain (e.g. electrical, fluidic, thermal). Each power flow has two power associated variables that can be referred to as an effort and a flow; the product of which is the power. Examples of the former are voltages and pressures, while examples of the latter are currents and volumetric flow rates. The power variables associated with each power flow on the SysML diagram can be distinguished as **independent** variables which are imposed on the function and **dependent** variables. Finally, mathematical models that express the dependent variables as functions of the independent variables are developed. As mentioned in Section I-E, the chosen models for each function are *first-pass* but *often-cited* engineering models. In the future, because the modeling strategy is very much modular, a practitioner may replace any of these functions with a more detailed physics-based model so long as it respects the high level functional interfaces. Alternatively, this modular modeling strategy can incorporate functional models developed through rigorous system identification.

The development of a transparent physics-based model for the energy-water nexus naturally brings about considerations of its practical implementation; both in physical modeling as well as numerical computation. In regards to physical modeling, there exist industrial grade multi-energy domain physical modeling software packages well-accepted by industry and academia alike. Dymola/Modelica [31], for example, has an active user community, lends itself to optimization problems [32] and has been demonstrated on models with over 100,000 equations [33]. Similarly, the General Algebraic Modeling System [34] provides an optimization-oriented modeling language. It's in-built nonlinear solvers have also been demonstrated on systems with over 100,000 equations [35].

Grid equations of the electricity, water and wastewater grids are modeled by means of edge-node incidence matrices. The remaining identified functions are developed using the bond graph methodology. The interested reader is referred to [36], [37] for an introduction to bond graph modelling.The bond graph methodology presents a number of practical advantages in this work. First, this methodology readily facilitates the inter-energy-domain modeling necessitated by the heterogeneous nature of the energy-water nexus. Next, it clearly distinguishes between the *directionality* found in the SysML activity diagrams and the *causality* of the associated quantitative models. As a result, it clarifies the dependence and independence of variables in the input-output model at the level of each individual function and thus ultimately for the full scope of the energy-water nexus model. This aspect is

particularly necessary to address the potential for closed loops of matter and energy. The bond graph methodology also allows the reuse of mathematical models within multiple functions as will be seen repeatedly with components such as pumps. Finally, the bond graph methodology facilitates the development of more complex models of the system functions either to incorporate previously neglected functionality or introduce dynamic effects.

C. Conventions of Modeling Notation

A wide range of variables across the three systems of interest are modelled in this work. The reader is referred to the nomenclature section for a full description of variables used in the models in Sections III, IV and V. As a general guide however, the convention used for the **power variables** is that boldface upper case letters are used to represent vector quantities and lower case letters are used to represent scalar quantities. For uniformity, this convention is followed even with variables for which it is common to represent scalar quantities with upper case letters; for example, lower case t is used to represent scalar temperatures rather than the more common upper case T . The letters used to represent the different power variables are as follows:

- $i \in \mathbf{I}$ - RMS Current
- $v \in \mathbf{V}$ - RMS Voltage
- $q \in \mathbf{Q}$ - Volumetric Flow Rate
- $p \in \mathbf{P}$ - Pressure
- $h \in \mathbf{H}$ - Specific Enthalpy
- $t \in \mathbf{T}$ - Temperature
- $m \in \mathbf{M}$ - Fuel consumption rate
- $\mathfrak{m} \in \mathfrak{M}$ -Steam mass flow rate

Additionally, the subscripts of these variables are denoted by the **set of facilities** to which they belong. Lower case subscripts are used for scalar quantities while boldface upper case subscripts are used for vector quantities:

- $f \in \mathbf{F}$ - Node in the water distribution network with known pressure (water treatment plant)
- $j \in \mathbf{J}$ - Node in water distribution network with unknown pressure
- $e \in \mathbf{E}$ - Node in non-potable recycled wastewater distribution network with unknown pressure
- $p \in \mathcal{P}$ - Water distribution link (includes both pipes and distribution pumps)
- $n \in \mathbf{N}$ - Non-potable recycled wastewater distribution link (includes both pipes and distribution pumps)
- $g \in \mathbf{G}$ - Generator
- $l \in \mathbf{L}$ - Electrical load
- $t \in \mathcal{T}$ - Electrical transmission line
- $w \in \mathbf{W}$ - Water source i.e. river, lake, aquifer or the sea
- $s \in \mathbf{S}$ - Water storage units, both tanks and artificial reserovirs
- $d \in \mathbf{D}$ - Wastewater treatment plant

III. Model of the Electricity System

Figure 3 shows the electricity system as a value chain. The four most prominent electricity generation technologies of thermal, hydroelectric, wind and solar PV are shown. These technologies have varying water withdrawal and consumption footprints. Thermal generation requires large volumes of water for cooling purposes and this requirement is one of the chief concerns associated with the energy-water nexus. Hydroelectric power requires flowing water to drive generating turbines. Solar panels and wind turbines have embedded water consumption due to their manufacturing processes but do not have any significant water requirements in operation. Bond graph models for each of these are developed below following the process in Figure 2.

A. Generate Electricity-Hydro

Independent Variables:p_w^{in}, p_w^{out}, i_g
Dependent Variables: q_g^{in}, q_g^{out}, v_g
Model function:

$$q_g^{in} = \mathfrak{f}_{hydro_{q^{in}}}([p_w^{in}, p_w^{out}, i_g])$$
$$q_g^{out} = \mathfrak{f}_{hydro_{q^{out}}}([p_w^{in}, p_w^{out}, i_g])$$
$$v_g = \mathfrak{f}_{hydro_{v}}([p_w^{in}, p_w^{out}, i_g])$$

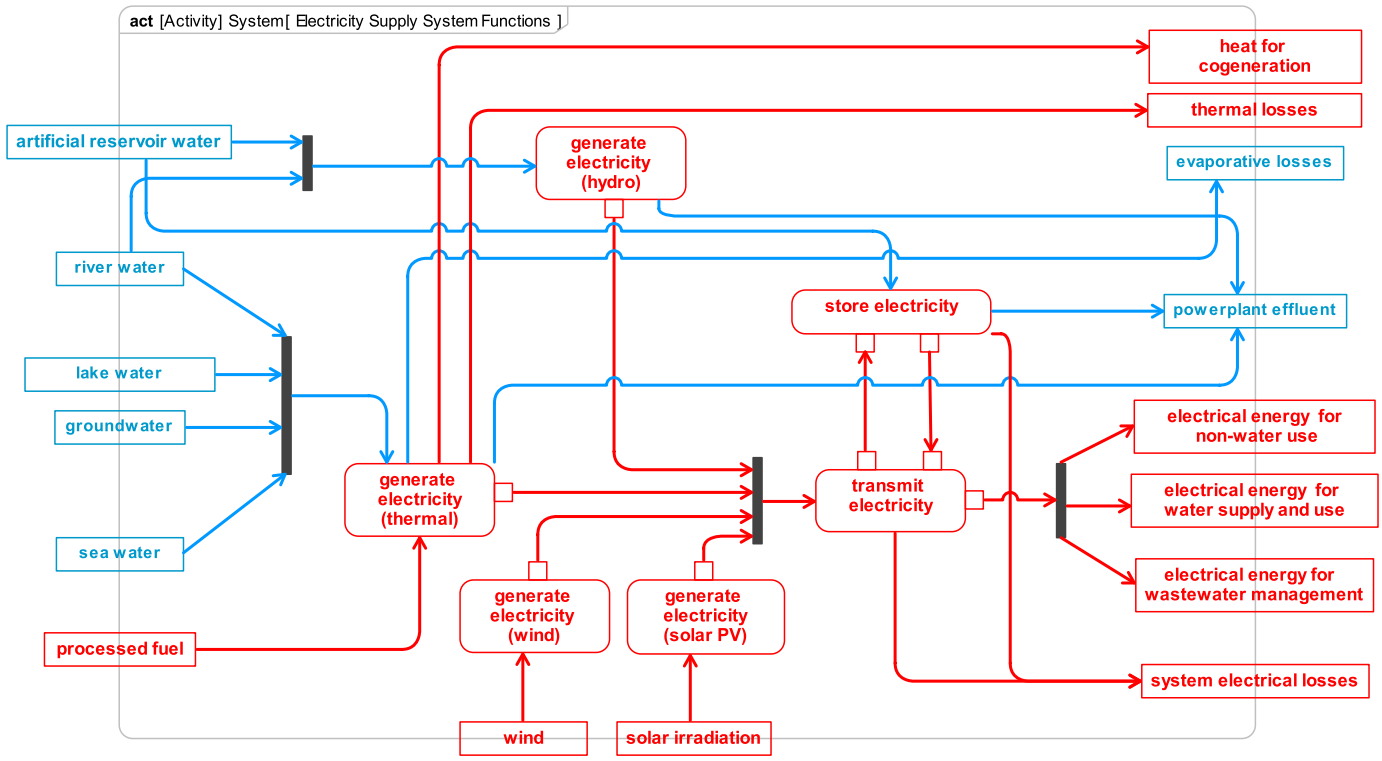

Fig. 3. Activity Diagram of Electricity System Functions

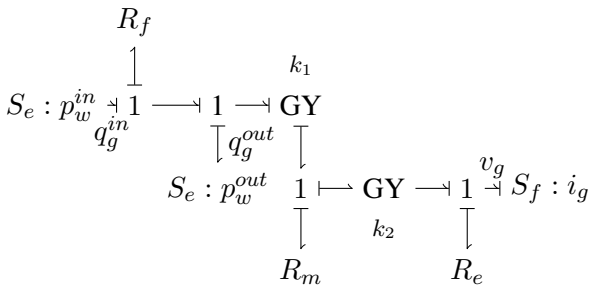

Fig. 4. Bondgraph representation of hydroelectric power generation.

Figure 4 shows a bond graph model of a hydroelectric power generation station maintaining the input and output interfaces of the associated activity in Figure 3. Water drawn from a reservoir at a pressure p_w^{in} drives a turbine that converts the hydraulic energy of the falling water into mechanical energy and that is represented in Figure 4 with an ideal gyrator of modulus k_1 as in [38]. The turbine, in turn, drives an AC generator for which a simple model presented in [36] is a gyrator modulated by the displacement of the rotor. As the interest in this work is not in the dynamic behaviour of this generator, this model is further simplified to an ideal gyrator with modulus k_2 as shown in the figure. Elements R_e, R_m and R_f represent resistances in the electrical, mechanical and fluidic domains.

Making the simplifying assumptions that the penstock resistance (R_f) is linear, and that there is no spillage ($q_g^{in} = q_g^{out} = q_g$), the voltage v_g generated by the power station and the water q_g withdrawn from the water source to drive generation can be determined as:

$$v_g = \left[\frac{k_1 k_2}{k_1^2 + R_m R_f}\right] p_w - \left[\frac{k_2 R_f}{k_1^2 + R_m R_f} + R_e\right] i_g \tag{1}$$

$$\left[\frac{R_m}{k_1 + R_f R_m}\right] p_w + \left[\frac{k_2}{k_1 + R_f R_m}\right] i_g \tag{2}$$

where $p_w = p_w^{in} - p_w^{out}$. The model in Figure 4 does not show the evaporative losses associated with hydroelectric generation. There does not exist any causality between the power generation process and these losses as the rate of evaporation from a particular reservoir will not be altered if the dam is generating below or at its full capacity. Furthermore, the water stored in the reservoir is often used not only for power generation but for water supply and thus the evaporation cannot be fully ascribed to electricity generation. The evaporative consumption is therefore best allocated to the reservoir as in Section IV-D and not to the power generation process .

B. Generate Electricity Thermal

Independent Variables: i_g, $\hbar_g$, t_w^{in}, t_w^{out}.
Dependent Variables: v_g, $\dot{m}_g$, q_g^{in},q_g^{out}
Model function:

$$\begin{aligned} v_g &= \mathfrak{f}_{thermal_v}([i_g, \hbar_g, t_w^{in}, t_w^{out}]) \\ \dot{m}_g &= \mathfrak{f}_{thermal_{\dot{m}}}([i_g, \hbar_g, t_w^{in}, t_w^{out}]) \\ q_g^{in} &= \mathfrak{f}_{thermal_{q^{in}}}([i_g, \hbar_g, t_w^{in}, t_w^{out}]). \\ q_g^{out} &= \mathfrak{f}_{thermal_{q^{out}}}([i_g, \hbar_g, t_w^{in}, t_w^{out}]) \end{aligned}$$

Many types of thermal power generation facilities exist today. They may be classified by fuel type (e.g. natural gas, coal, heavy fuel oil), cooling system type (once-through, semi-closed, closed-circuit), number of thermodynamic cycles (single, double, triple), and finally number of integrated products (e.g. electricity, steam, syngas) [39] Naturally, it is beyond the scope of this paper to present a model for all of these possible combinations. Rather, for the purposes of demonstrating the holistic nature of this work, a thermal generation facility is taken to be a single rankine cycle power plant with a once-through cooling system. Future work may introduce models for other types of thermal generation facilities as is deemed necessary.

Figure 5 shows a word bond graph for such a plant. The bonds internal to the cycle (shown in red) are convection bonds which have two effort variables and a single flow variable [37]. The flow variable is the mass flow rate of the steam, while the effort variables can be any two intensive properties —in this work the pressure and enthalpy are used as in [37].

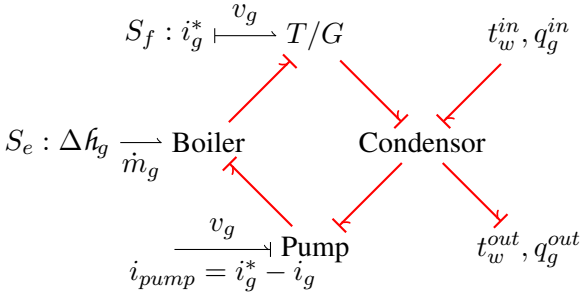

Fig. 5. Rankine Cycle Word Bond Graph

T/G in Figure 5 refers to the turbine and generator; i_g^* is the total current generated by the power plant, which is the sum of the current required by the pump and the current i_g drawn by the electrical network identified as an independent variable.

In order to develop an input-output model for thermal generation in the same manner as above for hydroelectric generation, it is helpful to develop individual input-output models for the different components of the rankine cycle and subsequently combine them. These models are presented in the following subsections. The models lean significantly on the convection bond graph concepts developed in [37]. The subscripts 1 to 4 used in the following subsections to represent different states of the process steam/water as follows:

(i) State 1 is the state of the process water at the condensor exit
(ii) State 2 is the state of the process water at the pump exit
(iii) State 3 is the state of the process steam at the boiler exit
(iv) State 4 is the state of the process steam at the turbine exit

It is assumed that there is a control system that ensures that the process water exiting the condensor is always saturated at a known temperature and pressure, that is to say that state 1 is a reference point for the rankine cycle. All other states vary with electric power demand. Each of the rankine cycle components is now discussed in turn taking into consideration that the dependent variables of an "upstream" component are the independent variables of the "downstream" component.

1) Component 1: Pump: **Independent Sub-variables:** Inlet pressure and specific enthalpy, p_1 ,h_1; Voltage applied to pump v_g
Dependent Sub-variables: Outlet pressure and specific enthalpy, p_2 ,h_2 ; Current drawn by pump i_{pump}
Component Model: A bond graph representation of the boiler feed pump, assumed isentropic, is shown in Figure 6. Typically a centrifugal pump is used [40], which is best represented by a modulated gyrator, (see Section IV-E), however a simple gyrator will be used here. The vertical bond from the 1-junction is a *simple* rather than convection bond with a single effort equal to the enthalpy difference between states 1 and 2; it allows connection of convection bond graphs to other parts of the system [37].

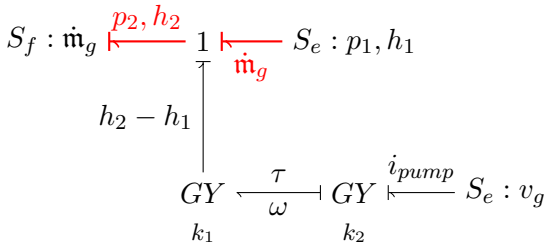

Fig. 6. Bondgraph representation of boiler feed pump

From the model, h_2 and the current i_{pump} are readily determined as:

$$\begin{aligned} h_2 &= h_1 + \frac{k_1}{k_2} v_g \\ i_{pump} &= \frac{k_1}{k_2} \nu_1 \ \dot{m}_g \end{aligned} \tag{3}$$

where ν_1 is the specific volume of the water (assumed saturated) entering the pump. Assuming incompressibility ($d\nu = 0$) and a negligible change in water temperature in the pump, it follows that $dh = \nu dP$. The outlet pressure p_2 is thus given by:

$$p_2 = p_1 + \frac{(h_2 - h_1)}{\nu_1} \tag{4}$$

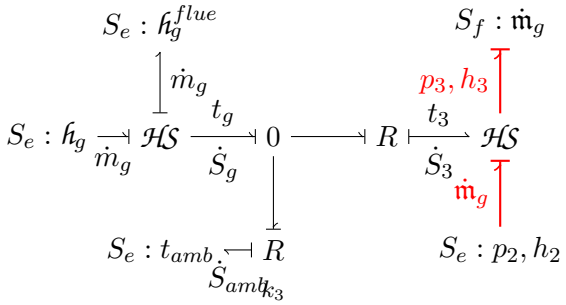

Fig. 7. Bondgraph representation of boiler

2) Component 2: Boiler: **Independent Sub-variables:** Inlet pressure and specific enthalpy, p_2 ,h_2; Lower heating value of fuel h_g
Dependent Sub-variables: Outlet pressure and specific enthalpy, p_3 ,h_3; Fuel consumption rate $\dot{m}_g$
Component Model:A bond graph of a boiler is presented in Figure 7. t_g and t_{amb} represent the boiler flame and

ambient temperatures respectively. Heat input to the boiler ($\dot{m}_g \hbar_g$) is lost through the flue gas and the boiler wall with the rest being usefully transferred to the process steam. The heat lost in the flue gas consists solely of sensible heat since the lower heating value of the fuel, $\hbar_g$ is used and thus the latent heat of the water vapour content of the flue gas has already been excluded. Mass of both the process steam and the fuel are conserved. The $\mathcal{HS}$ element represents a non-reversible heat exchanger [37] and is used here to represent the heat transfers from the fuel to the boiler wall, and from the boiler wall to the process steam. By conservation of energy, $\dot{m}_g$ is given by:

$$\dot{m}_g = \dot{\mathfrak{m}}_g \frac{(h_3 - h_2) + k_4(t_g - t_{amb})}{\hbar_g - \hbar_g^{flue}} \tag{5}$$

where k_3 is the thermal conductivity of the boiler-ambient interface and $\hbar_g^{flue}$ is the specific sensible heat content of the flue gas in J/kg which is a function of the specific heat capacity and temperature (approximately equal to t_g) of the flue gas. The right hand side of Equation 5 includes the unknown h_3 which can be determined with the aid of the turbine model below. There is no change in pressure in the boiler and thus the outlet pressure $p_3 = p_2$.

3) Component 3: Turbine: **Independent sub-variables:** Pressure of the inlet steam p_3; Current i_g^*
Dependent sub-variables: Pressure and specific enthalpy at the outlet p_4, h_4; Specific Enthalpy at the inlet, h_3; Voltage v_g
Component Model: Figure 8 shows a bond graph of the turbine assumed to be isentropic. As described above, the simple bond allows connection of convection bond graphs to other parts of the system [37], in this case a turbine, modeled as a displacement machine and thus represented by a transformer. The transformer modulus is a ratio ν_3/D where D is the volumetric displacement per radian of shaft rotation and ν_3 is the specific volume of the steam entering the machine [37]. The turbine shaft in turn drives a generator represented by a gyrator with modulus k_4. From the transformer and gyrator, it follows that:

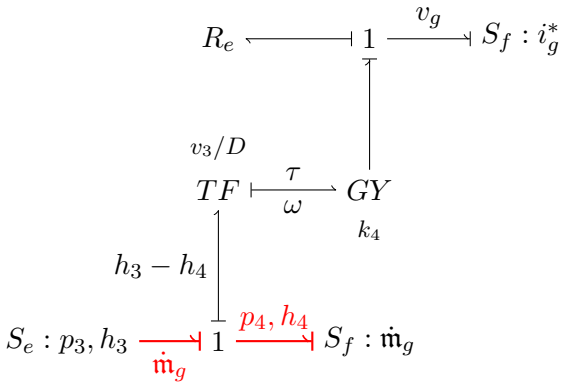

Fig. 8. Bondgraph representation of isentropic turbine

$$h_4 = h_3 - \frac{\nu_3 k_4}{D} i_g^* \tag{6}$$

$$v_g = \frac{\nu_3 k_4}{D} \dot{\mathfrak{m}}_g - R_e i_g^* \tag{7}$$

Given that the expansion is assumed to be isentropic and that $p_4 = p_1$ (there is no pressure drop in the condensor), the unknown h_3 in Equation 6 can be determined by simultaneously solving with the following equations:

$$\begin{aligned} s_3 &= s_4 \\ s_4 &= \mathfrak{f}_{s_4}(p_4, h_4) = \mathfrak{f}_{s_4}(p_1, h_4) \\ h_3 &= \mathfrak{f}_{h_3}(p_3, s_3) \end{aligned} \tag{8}$$

where $\mathfrak{f}_{s_4}$ and $\mathfrak{f}_{h_3}$ are polynomial regressions of appropriate portions of the superheated steam tables.

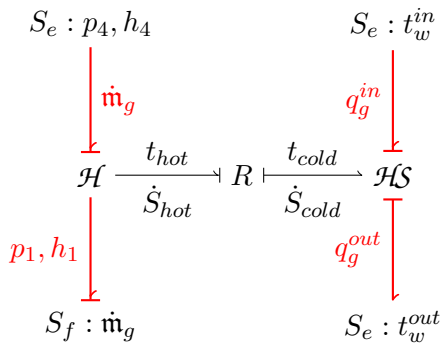

Fig. 9. Bondgraph representation of once-through condensor

4) Component 4: Condensor: **Independent sub-variables:** Inlet pressure and specific enthalpy p_4,h_4; Cooling water inlet temperature t_w^{in};Cooling water outlet temperature t_w^{out}
Dependent sub-variables: Outlet pressure and specific enthalpy, p_1,h_1 ; Cooling water withdrawal rate q_g^{in}; Cooling water effluent flow rate q_g^{out}
Component Model: Figure 9 is a bond graph representation of a once-through condensor using the $\mathcal{H}$, $\mathcal{HS}$, and two port resistance R elements. The $\mathcal{H}$ element represents an ideal, reversible heat exchanger [37]. The R element represents the condensor wall, a thermal resistance, across which heat is conducted to the cooling water.

The true effort variable associated with the cooling water volumetric flow rate is the specific enthalpy multiplied by the cooling water density, however since the cooling water is not subjected to a change of pressure or density in the condensor, changes in enthalpy are linearly related to changes in temperature. The use of temperature is particularly convenient because cooling water outlet temperature t_w^{out} is typically limited by regulation for ecosystem protection purposes, and t_w^{in} and t_w^{out} in Figure 5 can be replaced with a single effort variable Δt_w associated with the flow $q_g = q_g^{in} = q_g^{out}$. By conservation of energy:

$$q_g = \frac{\dot{\mathfrak{m}}_g (h_4 - h_1)}{\rho_w c_w \Delta t_w} \tag{9}$$

5) Combined Thermal Generation Model: The combined model for the thermal generation plant is thus given by:

$$v_g = \left(\frac{\nu_3 k_4}{D} - R_e \frac{k_1 \nu_1}{k_2} \right) \dot{\mathfrak{m}}_g - R_e i_g \tag{10}$$

$$q_g^{in} = q_g^{out} = q_g = \frac{\dot{\mathfrak{m}}_g}{\rho_w c_w \Delta t_w} (h_4 - h_1) \tag{11}$$

$$\dot{m}_g = \dot{\mathfrak{m}}_g \frac{(h_3 - h_2) + k_3 (t_g - t_{amb})}{h_g - h_g^{flue}} \tag{12}$$

where the specific enthalpies h_2, h_3, h_4 are determined by simultaneously solving Equations 3, 4, 6 and 8, and where Equation 10 is obtained by substituting for $i_g^* = i_g + i_{pump}$ in Equation 7.

C. Generate Electricity - Wind

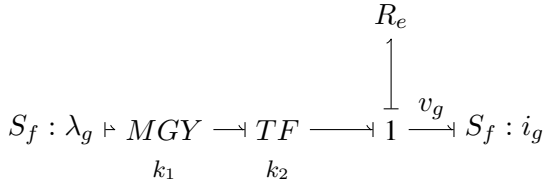

Fig. 10. Bondgraph model of wind turbine.

Independent Variables: λ_g, i_g
Dependent Variables: v_g. (The wind force corresponding to λ_g is not of interest and is thus not modelled.)
Model Function:

$$v_g = \mathfrak{f}_{wind_v}([\lambda_g, i_g])$$

Figure 10 is a simplified bond graph representation of a wind turbine. A more detailed model can be found in [41]. The gyrator is modulated by the windspeed, that is to say, the torque τ is a function of λ_g^2 [41]. The transformer is a combination of the generator and an inverter that effects change of causality from a current to a voltage. The generator voltage v_g is given by:

$$v_g = \frac{k_1}{k_2}\lambda_g^2 - i_g R_e \tag{13}$$

D. Generate Electricity - Solar photovoltaic

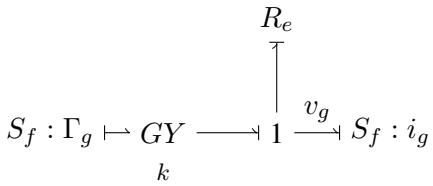

Fig. 11. Bond graph representation of solar PV installation

Independent Variables: Γ_g, i_g
Dependent Variables:v_g. (The voltage $v_g + i_g R_e$ imposed on the photocell is not of interest.)
Model Function:

$$v_g = \mathfrak{f}_{solar_v}([\Gamma_g, i_g])$$

A simple bond graph model of solar photovoltaic installationl previously presented in [4] is reproduced in Figure 11. The solar PV installation is approximated as a current source, a linear resistance, and a gyrator. In this model, the gyrator represents both the inverter switching circuit and the DC-to-DC conversion circuit. The function of the former is approximated by the change of causality from flow source to effort source effected by the gyrator while that of the latter is effected by the magnitude of the gyrator modulus. The resistance represents electrical losses in both processes.

From the model, the voltage v_g imposed on the electrical distribution network can be determined as:

$$v_g = \frac{\Gamma_g}{k} - i_g R_e \tag{14}$$

E. Transmit Electricity

Independent Variables: $\mathbf{V_G}$, $\mathbf{I_L}$
Dependent Variables: $\mathbf{I_G}$, $\mathbf{V_L}$
Model Function:

$$\mathbf{I_G} = \mathfrak{f}_{transmit_\mathbf{I}}([\mathbf{V_G}, \mathbf{I_L}])$$
$$\mathbf{V_L} = \mathfrak{f}_{transmit_\mathbf{V}}([\mathbf{V_G}, \mathbf{I_L}])$$

The transmission of electricity through an electricity distribution network is typically modelled in the phasor domain. We define the following phasor voltages and currents:

$$\begin{aligned} \mathcal{V}_\mathbf{G} &= \boldsymbol{\theta}_{\mathbf{V_G}} \mathbf{V_G} \\ I_\mathbf{G} &= \boldsymbol{\theta}_{\mathbf{I_G}} \mathbf{I_G} \\ \mathcal{V}_\mathbf{L} &= \boldsymbol{\theta}_{\mathbf{V_L}} \mathbf{V_L} \\ I_\mathbf{L} &= \boldsymbol{\theta}_{\mathbf{I_L}} \mathbf{I_L} \end{aligned} \tag{15}$$

where $\boldsymbol{\theta}_{\mathbf{V_G}}$, $\boldsymbol{\theta}_{\mathbf{V_L}}$,$\boldsymbol{\theta}_{\mathbf{I_G}}$,$\boldsymbol{\theta}_{\mathbf{I_L}}$ are diagonal $[G \times G]$matrices with entries of the form $1\angle\theta_i$, θ_i being the phase angle of the current or voltage at bus i. $\boldsymbol{\theta}_{\mathbf{V_G}}$, $\boldsymbol{\theta}_{\mathbf{I_L}}$ are assumed known. Two edge node-incidence matrices and one impedance matrix are also defined:

- Electrical load node incidence matrix $\mathbf{A_L}$ with dimensions $[\mathcal{T} \times L]$
- Generator node incidence matrix $\mathbf{A_G}$ with dimensions $[\mathcal{T} \times G]$
- Transmission line impedance matrix $\mathbf{R}_{\mathcal{T}}$ with dimensions $[\mathcal{T} \times \mathcal{T}]$

Kirchoff's Current Law and Ohm's law respectively provide the following equations:

$$\begin{aligned}\mathbf{A_L^\dagger} I_{\mathcal{T}} &= I_{\mathbf{L}}\\ \mathbf{A_G^\dagger} I_{\mathcal{T}} &= I_{\mathbf{G}}\\ \mathbf{A_G}\mathcal{V}_{\mathbf{G}} + \mathbf{A_L}\mathcal{V}_{\mathbf{L}} &= \mathbf{R}_{\mathcal{T}} I_{\mathcal{T}}\end{aligned}$$

These can be rearranged to yield:

$$\begin{aligned}\mathcal{V}_{\mathbf{L}} &= -\mathbf{A_1} I_{\mathbf{L}} + \mathbf{A_2}\mathcal{V}_{\mathbf{G}}\\ I_{\mathbf{G}} &= \mathbf{A_3} I_{\mathbf{L}} + \mathbf{A_4}\mathcal{V}_{\mathbf{G}}\end{aligned} \tag{16}$$

where

$$\begin{aligned}\mathbf{A_1} &= (\mathbf{A_L^\dagger R_{\mathcal{T}}^{-1} A_L})^{-1}\\ \mathbf{A_2} &= \mathbf{A_1 A_L^\dagger R_{\mathcal{T}}^{-1} A_G}\\ \mathbf{A_3} &= \mathbf{A_G^\dagger R_{\mathcal{T}}^{-1} A_L A_1}\\ \mathbf{A_4} &= \mathbf{A_G^\dagger R_{\mathcal{T}}^{-1} A_G} - \mathbf{A_G^\dagger R_{\mathcal{T}}^{-1} A_L A_1 A_L^\dagger R_{\mathcal{T}}^{-1} A_G}\end{aligned}$$

The † denotes the transpose of a matrix. $\mathbf{I_G}$ and $\mathbf{V_L}$ can then be determined as the RMS values of $I_{\mathbf{G}}$ and $\mathcal{V}_{\mathbf{L}}$ respectively. The RMS load current $\mathbf{I_L}$ can be decomposed into current drawn for water purposes and current drawn for all other purposes as in Figure 3:

$$\mathbf{I_L} = \mathbf{I_{L_0}} + \mathbf{C_{L\mathcal{P}} I_{\mathcal{P}}} + \mathbf{C_{LF} I_F} + \mathbf{C_{LD} I_D} \tag{17}$$

where $\mathbf{I_{L_0}}, \mathbf{I_{\mathcal{P}}}, \mathbf{I_F}, \mathbf{I_D}$ are as defined in the nomenclature (expressions to be derived in Sections IV and V) and are assumed to all be in phase; and $\mathbf{C_{L\mathcal{P}}}, \mathbf{C_{LF}}, \mathbf{C_{LD}}$ are binary coupling matrices such that $\mathbf{C_{L\mathcal{P}}}(l,p) = 1$, $\mathbf{C_{LF}}(l,f) = 1$ and $\mathbf{C_{LD}}(l,d) = 1$ if pump p, water treatment plant f, and wastewater treatment plant d respectively are connected to electrical load node l.

F. Summary of Electricity System Function Models

Writing the model functions defined in Sections III-A, III-B, III-C, III-D and III-E in matrix form we have a combined model for the electricity system functions identified in Figure 3:

$$\begin{aligned}\mathbf{V_G} =& \mathfrak{f}_{\mathbf{hydro_V}}([\mathbf{P_W}, \mathbf{I_G}]) + \mathfrak{f}_{\mathbf{thermal_V}}[\mathbf{I_G}, \mathcal{H}_{\mathbf{G}}, \Delta\mathbf{T_W}] +\\ & \mathfrak{f}_{\mathbf{wind_V}}(\boldsymbol{\lambda}_{\boldsymbol{G}}, \mathbf{I_G}]) + \mathfrak{f}_{\mathbf{solar_V}}([\boldsymbol{\Gamma}_{\boldsymbol{G}}, \mathbf{I_G}])\\ \mathbf{Q_G}^{in} =& \mathfrak{f}_{\mathbf{hydro_{Q^{in}}}}([\mathbf{P_W}, \mathbf{I_G}]) + \mathfrak{f}_{\mathbf{thermal_{Q^{in}}}}[\mathbf{I_G}, \mathcal{H}_{\mathbf{G}}, \Delta\mathbf{T_W}]\\ \mathbf{Q_G}^{out} =& \mathbf{Q_G}^{in} - \mathbf{Q_G}^{evap}\\ \dot{\mathbf{M}}_{\mathbf{G}} =& \mathfrak{f}_{\mathbf{thermal_{\dot{M}}}}[\mathbf{I_G}, \mathcal{H}_{\mathbf{G}}, \Delta\mathbf{T_W}]\\ \mathbf{I_G} =& \mathfrak{f}_{\mathbf{transmit_I}}([\mathbf{V_G}, \mathbf{I_L}])\\ \mathbf{V_L} =& \mathfrak{f}_{\mathbf{transmit_V}}([\mathbf{V_G}, \mathbf{I_L}])\end{aligned} \tag{18}$$

For the particular case of the models developed in each of the preceeding sections, Equation 18 can be instantiated with Equations 1, 2 10, 11, 12, 13 and 14 written in matrix form :

$$\begin{aligned}\mathbf{V_G} &= \mathbf{K_1} + \mathbf{K_2 C_{GW} P_W} + \mathbf{K_3}\boldsymbol{\lambda}_{\boldsymbol{G}} + \mathbf{K_4}\boldsymbol{\Gamma}_{\boldsymbol{G}} - \mathbf{K_5 I_G}\\ \mathbf{Q_G}^{in} &= \mathcal{F}_{\mathbf{G_1}}(\mathbf{I_G}, \mathbf{C_{GW}}\Delta\mathbf{T_W})\\ \mathbf{Q_G}^{out} &= \mathbf{Q_G}^{in} - \mathbf{Q_G}^{evap}\\ \dot{\mathbf{M}}_{\mathbf{G}} &= \mathcal{F}_{\mathbf{G_2}}(\mathbf{I_G}, \mathcal{H}_{\boldsymbol{G}})\\ \mathbf{V_L} &= RMS(\mathbf{A_1}\boldsymbol{\theta}_{\mathbf{I_L}}\mathbf{I_L} - \mathbf{A_2}\boldsymbol{\theta}_{\mathbf{V_G}}\mathbf{V_G})\\ \mathbf{I_G} &= RMS(\mathbf{A_3}\boldsymbol{\theta}_{\mathbf{I_L}}\mathbf{I_L} + \mathbf{A_4}\boldsymbol{\theta}_{\mathbf{V_G}}\mathbf{V_G})\end{aligned} \tag{19}$$

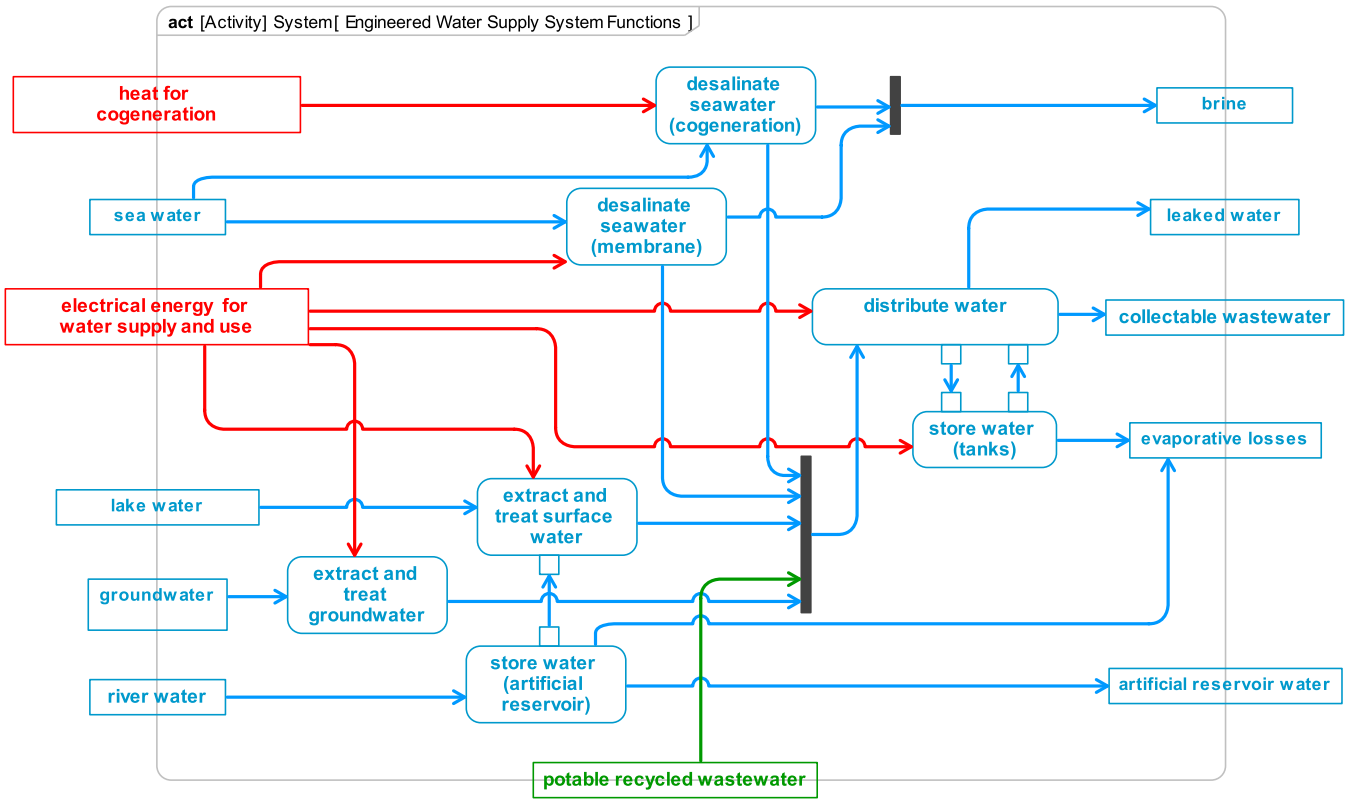

Fig. 12. Activity Diagram of Water System Functions

where $\mathbf{C_{GW}}$ is a binary coupling matrix such that $\mathbf{C_{GW}}(g,w) = 1$ if generator g is connected to water source w. $\mathbf{K_1}$ is a $[G \times 1]$ vector whose value $\mathbf{K_1}(g)$ is given by Equation 10 for all thermal power generators g. Similarly, $\mathbf{K_2}, \mathbf{K_3}, \mathbf{K_4}$ are $[G \times G]$ diagonal matrices with diagonal elements $\mathbf{K_2}(g,g)$, $\mathbf{K_3}(g,g)$, $\mathbf{K_4}(g,g)$, given by Equations 1, 13 and 14 for all hydroelectric, wind, and solar power plants respectively. $\mathbf{K_5}(g,g)$ represents the electrical losses of each power plant g and is given by Equations 1, 10, 13 and 14 depending on the type of plant. $\mathcal{F}_{\mathbf{G_1}}$ and $\mathcal{F}_{\mathbf{G_2}}$ are vector functions with $f_{\mathbf{g_1}}(g)$ and $f_{\mathbf{g_2}}(g)$ given by Equations 11 and 12 respectively for all thermal generators g.

IV. Model of the Engineered Water Supply System

An activity diagram for the engineered water supply system is shown in Figure 12. All water grid functions are dependent on electrical or thermal energy input. Pumping, either for extraction or distribution, is responsible for the bulk of electrical energy consumed by the water system. Thermal desalination, typically in the form of cogeneration plants that produce both water and electricity, is driven by thermal energy input. Models of the four indicated water supply options are presented below. Electricity consumption for municipal water use is not modelled as it represents a plethora of different processes that are typically not under the purview of grid operators.

A. Extract and treat ground water and surface water

Independent Variables: q_f,p_w,v_f
Dependent Variables: p_f, q_w,i_f.
Model Function:

$$p_f = \mathfrak{f}_{treat_p}([q_f, p_w, v_f])$$
$$q_w = \mathfrak{f}_{treat_q}([q_f, p_w, v_f])$$
$$i_f = \mathfrak{f}_{treat_i}([q_f, p_w, v_f])$$

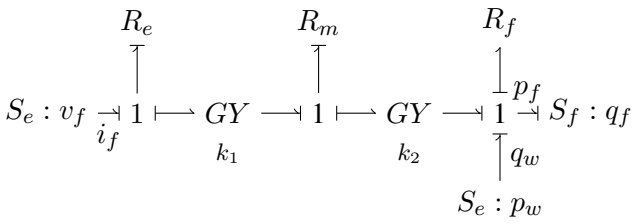

Fig. 13. Bondgraph representation of surfacewater /groundwater treatment plant.

The extraction and treatment of surface and ground water can be effectively modelled as a pump as pumping consumes atleast 98 percent of the power at each treatment plant [15]. A bond graph representation of a treatment plant as a centrifugal pump driven by an electric motor is shown in Figure 13. The following input-output equations are derived from the model:

$$q_w = q_f \tag{20}$$

$$i_f = \frac{k_1 k_2}{k_1^2 + R_m R_e} q_f + \frac{R_m}{k_1^2 + R_m R_e} v_f \tag{21}$$

$$p_f = -\left[\frac{k_1^2 + R_e R_m + k_2 R_e}{k_1^2 + R_e R_m}\right] q_f + \frac{k_1 k_2}{k_1^2 + R_e R_m} v_f + p_w \tag{22}$$

B. Desalinate Seawater (Cogeneration)

Independent Variables:Distillate demand from water distribution network q_f, Temperature of feed water t_w,Heating steam flow rate $\dot{\mathfrak{m}}$

Dependent Variables: Enthalpy drop Δh of heating steam, Brine Output q_f^{brine}, Feed water withdrawal rate q_w

Model Function:

$$\begin{aligned} \Delta h &= \mathfrak{f}_{desalC_h}([q_f, t_w, \dot{\mathfrak{m}}]) \\ q_f^{brine} &= \mathfrak{f}_{desalC_{q^{brine}}}([q_f, t_w, \dot{\mathfrak{m}}]) \\ q_w &= \mathfrak{f}_{desalC_q}([q_f, t_w, \dot{\mathfrak{m}}]) \end{aligned}$$

Multistage flash (MSF) desalination, the dominant thermal desalination process is typically integrated with thermal generation in cogeneration plants as shown in Figure 14 with the desalination process deriving its requisite thermal energy from steam extracted from a back pressure turbine at the appropriate specific enthalpy to drive the desalination process [42]–[44].

Focusing on the flash desalination unit in Figure 14 —the models for the other units are unchanged from Subsection III-B as discussed below —a model of the desalination process can be developed following the procedure in Figure 2.

Figure 15 is a bond graph representation of a flash desalination plant. Typically these plants consist of multiple stages of successively lower pressures and temperatures, however, as a simplification, a single stage flash desalination plant is modelled in Figure 15.

It is of interest to determine the enthalpy drop Δh of the heating steam. From the bond graph, assuming that there is no accummulation of vapour or liquid in the flashing stage, Δh can be determined as:

$$\Delta h = q_f Z \tag{23}$$

where $Z = \left[\rho\, h_v^{stg}(t^{stg} - t_w)\right] / \left[\dot{\mathfrak{m}}\, \Delta t^{stg}\right]$. h_v^{stg} is the vaporization enthalpy at the stage temperature t^{stg}, ρ is the distillate density, and Δt^{stg} is the temperature drop across the flashing stage.

In order to determine the brine output, an average recovery ratio [43] will be used:

$$q_f^{brine} = \frac{1 - RR}{RR} q_f \tag{24}$$

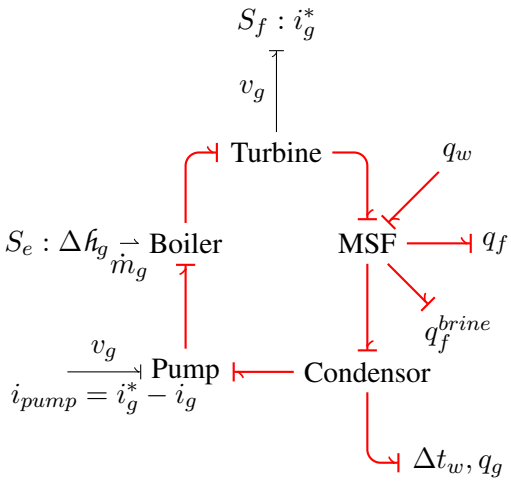

Fig. 14. Word Bond Graph of MSF plant integrated with Rankine Cycle

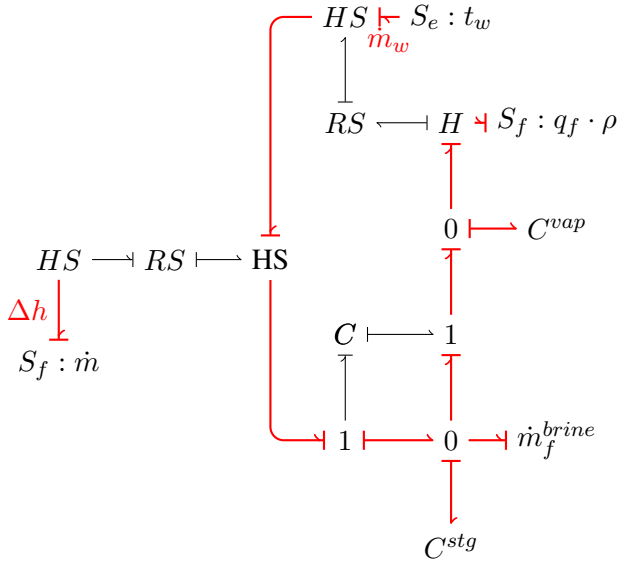

Fig. 15. Bondgraph representation of a thermal (flash) desalination plant.

The feedwater withdrawal rate q_w is therefore:

$$q_w = \frac{q_f}{RR} \tag{25}$$

As stated, thermal desalination is typically integrated with thermal power generation in a cogeneration plant. In this setup, the heating steam is taken from the exit of a back-pressure turbine and is superheated. It can be reasonably assumed that the enthaply of the steam exiting the desalination unit is always greater than h_1 in Section III-B, that is, it is a saturated mixture. A condenser is therefore still required and the desalination unit can be thought of as utilizing 'waste heat'. There is therefore no increase in fuel consumption due to the addition of the desalination unit and fuel consumption is still given by Equation 12. The voltage v_g generated by the power generation cycle of the cogeneration plant as given by Equation 7 is also unchanged. The cooling water requirement for the cogeneration plant is reduced as some of the waste heat is used for the desalination process instead of being injected into the cooling water. This cooling requirement q_g is readily determined by comparison with Equation 9 as:

$$q_g = \frac{\rho_w \dot{\mathfrak{m}}(h_2 - Zq_f - h_3)}{c_w \Delta t_w} \tag{26}$$

where Z is the coefficient identified in Equation 23. Note that in the case of a cogeneration plant, this cooling water is abundantly available sea water. The primary concern from an energy water nexus perspective of these withdrawals is therefore the long term effect of the returned water at an elevated temperature on marine ecosystems. Conversely, when the source is fresh water, there is an added concern of the vulnerability of power plant operations to fresh water scarcity. Ultimately, there is a trade-off between increased water temperatures Δt_w and the freshwater requirement q_g.

C. Desalinate Seawater (Membrane)

Independent Variables: q_f, p_w, v_f
Dependent Variables: p_f, q_w, i_f, q_f^{brine}
Model Function:

$$\begin{aligned} p_f &= \mathfrak{f}_{desalM_p}([q_f, p_w, v_f]) \\ q_w &= \mathfrak{f}_{desalM_q}([q_f, p_w, v_f]) \\ i_f &= \mathfrak{f}_{desalM_i}([q_f, p_w, v_f]) \\ q_f^{brine} &= \mathfrak{f}_{desalM_{q^{brine}}}([q_f, p_w, v_f]) \end{aligned}$$

A reverse osmosis plant is similar to surface and ground water treatment plants except that additional electrical energy is drawn to overcome the osmotic pressure π_w, a parameter of the seawater. As a first approximation i_f can be given by:

$$i_f = \frac{k_1 k_2}{k_1^2 + R_m R_e} q_f + \frac{R_m}{k_1^2 + R_m R_e} v_f + k_5 \pi_w \tag{27}$$

Including brine output in a bond graph model of a reverse osmosis desalination plant would have necessitated the development of chemical bond graphs, a level of detail considered unnecessary for this work. Instead, as in Section a typical recovery ratio, RR can be used to determine the brine output:

$$q_f^{brine} = \frac{1 - RR}{RR} q_f \tag{28}$$

The feedwater withdrawal rate q_w is therefore:

$$q_w = \frac{q_f}{RR} \tag{29}$$

D. Store Water (Tanks and Artificial Reservoirs)

Independent Variables: $\mathbf{Q_S}$(artificial reservoirs), $\mathbf{Q_S}^{evap}$
Dependent Variables: $\mathbf{Q_S}$(tanks),$\mathbf{Q_W}$

The two water storage functions in Figure 12 are treated together. For tanks it is desired to have a model of the form $\mathbf{Q_S} = \mathfrak{f}_{store1}(\mathbf{Q_S^{evap}})$ and for artificial reservoirs it is desired to have a model of the form $\mathbf{Q_W} = \mathfrak{f}_{store2}(\mathbf{Q_S})$. Let $\boldsymbol{\mu_S}(t)$ be an $[S \times 1]$ vector of the quantities of water stored in a tank or artificial reservoir at a time t. Changes in this quantity of water are related to water injections into or out of the storage unit from the water distribution system in the case of tanks and from upstream users in the case of artificial reservoirs $\mathbf{Q_S}$, evaporation losses $\mathbf{Q_S}^{evap}$ and water withdrawals from a water source $\mathbf{Q_W}$ as follows:

$$\boldsymbol{\mu_S}(t + \Delta t) = \boldsymbol{\mu_S}(t) + \Delta t(\mathbf{Q_S} - \mathbf{Q_S}^{evap} + \mathbf{C_{SW}} \mathbf{Q_W}) \tag{30}$$

where $\mathbf{C_{SW}}$ is a binary coupling matrix such that $\mathbf{C_{SW}}(s, w) = 1$ if artificial reservoir s withdraws water from water source w. Equation 30 can be recast for tanks as follows:

$$\mathbf{Q_S} = \mathbf{Q_S}^{evap} + (\boldsymbol{\mu_S}(t + \Delta t) - \boldsymbol{\mu_S}(t))/\Delta t \tag{31}$$

where $\mathbf{Q_S}$ appears as a demand that can take on postivie and negative values in water distribution system as shown in Section IV-E. Similarly, Equation 30 can be recast for artificial reservoirs as:

$$\mathbf{Q_W} = \mathbf{C_{WS}}(\mathbf{Q_S} + \mathbf{Q_S}^{evap} + (\boldsymbol{\mu_S}(t + \Delta t) - \boldsymbol{\mu_S}(t))/\Delta t) \tag{32}$$

In the case of the artificial reservoir, $\mathbf{Q_S}$ is an independent variable determined by upstream uses such as water treatment plants or hydroelectric power plants.

E. Distribute Water

Independent Variables: $\mathbf{P_F}$, $\mathbf{Q_J}$, $\mathbf{V}_{\mathcal{P}}$, p_{atm}, $\mathbf{Q_S}$, $\mathbf{Q_S}^{evap}$
Dependent Variables:$\mathbf{Q_F}$, $\mathbf{P_J}$, $\mathbf{I}_{\mathcal{P}}$,$\mathbf{Q_{Jl}}$.
Model Function: **Model Function**:

$$[\mathbf{Q_F}, \mathbf{P_J}, \mathbf{I}_{\mathcal{P}}, \mathbf{Q_{Jl}}] = \mathfrak{f}_{\mathbf{distribute}}([\mathbf{P_F}, \mathbf{Q_J}, \mathbf{V}_{\mathcal{P}}, \mathbf{Q_S}, \mathbf{Q_S^{evap}}])$$

The distribution of water through a pipe network can be easily described with the aid of two edge node-incidence matrices and one resistance matrix:

- Interior node incidence matrix $\mathbf{B_J}$ with dimensions $[\mathcal{P} \times J]$
- Fixed pressure node incidence matrix $\mathbf{B_F}$ with dimensions $[\mathcal{P} \times F]$
- Diagonal pipe and pump resistance matrix $\mathbf{R}_{\mathcal{P}}$ with dimensions $[\mathcal{P} \times \mathcal{P}]$

As the pressure loss due to the resistance of water pipes and pressure gain due to pumps are both non-linear functions of the flow rate, in the equations below, the dependent variable $\mathbf{Q_F}$ is replaced with with the more computationally convenient pipe and pump flow rates $\mathbf{Q}_{\mathcal{P}}$ as is customary in water distribution network analysis [45]. $\mathbf{Q_F}$ is then given by $\mathbf{B_F}^{\dagger}\mathbf{Q}_{\mathcal{P}}$.

Leakages occur in pipes but are typically allocated to nodes as pressure-dependent demands for modelling purposes [45], [46]. A simple model, in which the node is treated as an orifice through which the leakage Q_{jl} is discharged [46] provides the relationship:

$$q_{jl} = \beta_j p_j^{\alpha_j}$$

where β_j and α_j are nodal parameters.Therefore, in matrix form, the nodal leakages are determined as follows:

$$\mathbf{Q_{J_l}} = \boldsymbol{\beta_J}(\mathbf{P_J})\mathbf{P_J} \tag{33}$$

where $\boldsymbol{\beta_J}$ is a $[J \times J]$ diagonal matrix with entries $\beta_j P_j^{\alpha_j - 1}$.

By continuity of mass, the previously discussed allocation of node leakages and the integration of storage as discussed in Section IV-D, the interior nodes (**J**) are described by:

$$\mathbf{B_J}^{\dagger}\mathbf{Q}_{\mathcal{P}} + \mathbf{Q_J} + \mathbf{Q_{J_l}} + \mathbf{C_{JS}}(\mathbf{Q_S} + \mathbf{Q_S}^{evap}) = 0 \tag{34}$$

The constitutive equations for the pipes and pumps provide:

$$\mathbf{R}_{\mathcal{P}}(\mathbf{Q}_{\mathcal{P}})\mathbf{Q}_{\mathcal{P}} - \mathbf{B_J}\mathbf{P_J} - \mathbf{B_F}\mathbf{P_F} = 0 \tag{35}$$

Finally, in order to determine the current drawn by the pumps in the hydraulic network, a model of a centrifugal pump is required such as the one in Figure 16.

$$S_e : v_p \xrightarrow[i_p]{} GY \underset{k_p}{} \xrightarrow[\omega]{\tau} MGY \underset{\psi_1 + \psi_2 q_p}{} \xrightarrow[q_p]{\Delta p_p}$$

Fig. 16. Bondgraph representation of centrifugal pump

A centrifugal pump can be modelled as a modulated gyrator with modulus $\psi_1 + \psi_2 q$ [47] driven by an electric motor. The current drawn therefore is given by:

$$i_p = k_p(\psi_1 + \psi_2 q_p)q_p \tag{36}$$

In matrix form, this can be written as:

$$\mathbf{I}_{\mathcal{P}} = \mathbf{K}_{\mathcal{P}}\boldsymbol{\Psi}_{\mathcal{P}}(\mathbf{Q}_{\mathcal{P}})\mathbf{Q}_{\mathcal{P}} \tag{37}$$

where $\mathbf{K}_{\mathcal{P}}$ and $\boldsymbol{\Psi}_{\mathcal{P}}$ are $[\mathcal{P} \times \mathcal{P}]$ diagonal matrices with entries $\mathbf{K}_{\mathcal{P}}(p,p)$ and $\boldsymbol{\Psi}_{\mathcal{P}}(p,p)$ given by Equation 36 for each pump p.

$$\begin{bmatrix} \boldsymbol{\beta_J}(\mathbf{P_J}) & 0 & \mathbb{1}_{\mathbf{J}} & 0 \\ 0 & 0 & \mathbb{1}_{\mathbf{J}} & \mathbf{B_J}^{\dagger} \\ \mathbf{B_J} & 0 & 0 & -\mathbf{R}_{\mathcal{P}}(\mathbf{Q}_{\mathcal{P}}) \\ 0 & \mathbb{1}_{\mathcal{P}} & 0 & -\mathbf{K}_{\mathcal{P}}\boldsymbol{\Psi}_{\mathcal{P}}(\mathbf{Q}_{\mathcal{P}}) \end{bmatrix} \begin{bmatrix} \mathbf{P_J} \\ \mathbf{I}_{\mathcal{P}} \\ \mathbf{Q_{J_1}} \\ \mathbf{Q}_{\mathcal{P}} \end{bmatrix} + \begin{bmatrix} 0 \\ \mathbf{Q_J} + \mathbf{C_{JS}}(\mathbf{Q_S} + \mathbf{Q_S}^{evap}) \\ \mathbf{B_F P_F} \\ 0 \end{bmatrix} = \begin{bmatrix} 0 \\ 0 \\ 0 \\ 0 \end{bmatrix} \tag{39}$$

$$\begin{aligned} \mathbf{Q_F} &= \mathbf{B_F}^{\dagger}\mathbf{Q}_{\mathcal{P}} \\ \mathbf{I_F} &= \mathbf{K_6}\mathbf{Q_F} + \mathbf{K_7}\mathbf{V_F} + \mathbf{K_8}\mathbf{C_{WF}}^{\dagger}\boldsymbol{\Pi_W} \\ \mathbf{P_F} &= \mathbf{K_9}\mathbf{Q_F} + \mathbf{K_{10}}\mathbf{V_F} + \mathbf{C_{WF}}^{\dagger}\mathbf{P_W} \\ \Delta\mathbf{H_F} &= \mathbf{Z_F}\mathbf{Q_F} \end{aligned}$$

F. Summary of Engineered Water Supply System Equations

Writing the model functions defined in Sections IV-A, IV-C, IV-C and IV-E in matrix form we have a combined model for the water system functions identified in Figure 12:

$$\begin{aligned} (\mathbf{Q_F}, \mathbf{P_J}, \mathbf{I}_{\mathcal{P}}, \mathbf{Q_{Jl}}) &= \mathfrak{f}_{\mathbf{distribute}}([\mathbf{P_F}, \mathbf{Q_J}, \mathbf{V}_{\mathcal{P}}, \mathbf{Q_S}, \mathbf{Q_S^{evap}}]) \\ \mathbf{I_F} &= \mathfrak{f}_{\mathbf{treat_I}}([\mathbf{Q_F}, \mathbf{P_W}, \mathbf{V_F}]) + \mathfrak{f}_{\mathbf{desalM_I}}([\mathbf{Q_F}, \mathbf{P_W}, \mathbf{V_F}]) + \\ &\quad \mathfrak{f}_{\mathbf{desalC_I}}([\mathbf{Q_F}, \mathbf{P_W}, \mathbf{V_F}]) \\ \mathbf{P_F} &= \mathfrak{f}_{\mathbf{treat_P}}([\mathbf{Q_F}, \mathbf{P_W}, \mathbf{V_F}]) + \mathfrak{f}_{\mathbf{desalM_P}}([\mathbf{Q_F}, \mathbf{P_W}, \mathbf{V_F}]) + \\ &\quad \mathfrak{f}_{\mathbf{desalC_P}}([\mathbf{Q_F}, \mathbf{P_W}, \mathbf{V_F}]) \\ \Delta\mathbf{H_F} &= \mathfrak{f}_{\mathbf{desalC_H}}([\mathbf{Q_F}, \mathbf{T_W}, \dot{\mathfrak{M}}]) \\ \mathbf{Q_F}^{brine} &= \mathfrak{f}_{\mathbf{desalC_{Qbrine}}}([\mathbf{Q_F}, \mathbf{T_W}, \dot{\mathfrak{M}}]) \\ \mathbf{Q_W} &= \mathfrak{f}_{\mathbf{desalC_q}}([\mathbf{Q_F}, \mathbf{T_W}, \dot{\mathfrak{M}}]) \end{aligned} \tag{38}$$

For the particular case of the models developed in each of the preceeding subsections, Equation 38 can be instantiated with the scalar Equations 20, 21, 22, 23, 27 written in matrix form and combined with Equations 33, 34, 35 and 37, to yield the system in Equation 39, where $\mathbb{1}_{\mathbf{J}}$ and $\mathbb{1}_{\mathcal{P}}$ are $[\mathbf{J} \times \mathbf{J}]$ and $[\mathcal{P} \times \mathcal{P}]$ identity matrices respectively; $\mathbf{C_{WF}}$ is a binary coupling matrix such that $\mathbf{C_{WF}}(w, f) = 1$ if water from source w is withdrawn by treatment plant f; $\mathbf{K_6}, \mathbf{K_7}$ and $\mathbf{K_8}$ are $[\mathbf{F} \times \mathbf{F}]$ diagonal matrices with entries $\mathbf{K_6}(f, f)$, $\mathbf{K_7}(f, f)$ and $\mathbf{K_8}(f, f)$ given by the coefficients derived in Equation 27 for all surfacewater, groundwater and reverse osmosis plants f; $\mathbf{K_9}$ and $\mathbf{K_{10}}$ are are $[\mathbf{F} \times \mathbf{F}]$ diagonal matrices with entries $\mathbf{K_9}(f, f)$, and $\mathbf{K_{10}}(f, f)$ given by the coefficients derived in Equation 22 for all surfacewater, groundwater and reverse osmosis plants f; and where $\mathbf{Z_F}$ is an $[\mathbf{F} \times \mathbf{F}]$ diagonal matrix with entries $\mathbf{Z_F}(f, f)$ given by the coefficient derived in Equation 23 for each cogeneration plant f.

V. Model of the Wastewater System

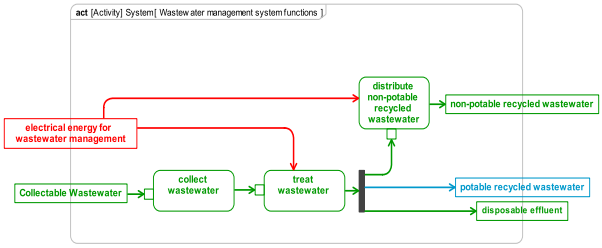

Fig. 17. Activity Diagram of Wastewater Functions

Figure 17 is an activity diagram of wastewater system functions. As in the previous sections, the strategy in Figure 2 will be followed.

A. Collect Wastewater

Independent Variables: $\mathbf{Q_J}$
Dependent Variables: $\mathbf{Q_D}$
Model Function:

$$\mathbf{Q_D} = \mathfrak{f}_{collectWW}(\mathbf{Q_J})$$

Wastewater collection, as shown in Fig. 17, typically does not require electric power input. Wastewater is typically conveyed by gravity-flow sewers [7] as wastewater treatment plants are built at low elevations, close to the water bodies into which effluent is to be discharged. The sewer hydraulics will thus be ignored in this model and the collection represented by a simple mass balance:

$$\mathbf{Q_D} = \mathbf{C_{DJ}}\mathbf{Q_J} \tag{40}$$

where $\mathbf{C_{DJ}}$ is a binary coupling matrix with $\mathbf{C_{DJ}}(d, j) = 1$ if wastewater treatment plant d treats wastewater from water demand node j.

B. Treat Wastewater

Independent Variables: $\mathbf{Q_D}$, $\mathbf{Q_F}$, $\mathbf{Q_D}^{rec}$
Dependent Variables: $\mathbf{I_D}$, $\mathbf{Q_D}^{disp}$
Model Function:

$$\mathbf{I_D} = \mathfrak{f}_{treatWW_I}([\mathbf{Q_D}, \mathbf{Q_F}, \mathbf{Q_D}^{rec}])$$
$$\mathbf{Q_D}^{disp} = \mathfrak{f}_{treatWW_Q}([\mathbf{Q_D}, \mathbf{Q_F}, \mathbf{Q_D}^{rec}])$$

Electrical energy is required for the treatment of wastewater and distribution of recycled wastewater. Bond graphs can be used to model chemical reactions [48] such as biochemical processes found in wastewater treatment facilities [49]. However, as *first-pass* models are desirable to limit the complexity of this research, an approximation is made such that the current drawn by wastewater treatment linearly depends on the volume flow rate of the water it treats. This is reasonable as power system voltages are typically maintained close to 1.0 per unit and thus often reported empirical measures of energy consumption per unit volume of treated water [49] can be related to electric current demand:

$$\mathbf{I_D} = \mathbf{K_D}\mathbf{Q_D} \tag{41}$$

where $\mathbf{K_D}$ is a $[D \times D]$ diagonal matrix consisting of the described linear factors. The treated wastewater may be recycled, as indicated in Figure 17, through a dedicated non-potable recycled wastewater distribution network (Section V-C), or blended into the potable water distribution network in which case the wastewater recycling plant doubles as a water supply plant in Section IV. The water that is not recycled and that is thus directly returned to a water source $\mathbf{Q_D}^{disp}$ is given by:

$$\mathbf{Q_D}^{disp} = \mathbf{Q_D} - \mathbf{C_{DF}}\mathbf{Q_F} - \mathbf{Q_D}^{rec} \tag{42}$$

where $\mathbf{C_{DF}}$ is a binary coupling matrix with $\mathbf{C_{DF}}(d, f) = 1$ if wastewater treatment plant d doubles as water supply plant f, $\mathbf{Q_D}^{rec}$ is the water recycled through a dedicated non-potable recycled wastewater distribution network (Section V-C) and $\mathbf{Q_F}$ is as previously determined in Section IV-E.

C. Distribute Non-Potable Recycled Wastewater

Independent Variables: $\mathbf{P_D}$, $\mathbf{Q_E}$, $\mathbf{V_N}$, p_{atm}
Dependent Variables: $\mathbf{Q_D}^{rec}$, $\mathbf{P_E}$, $\mathbf{I_N}$,$\mathbf{Q_{El}}$.
Model Function:

$$[\mathbf{Q_D}^{rec}, \mathbf{P_E}, \mathbf{I_N}, \mathbf{Q_{El}}] = \mathfrak{f}_{\mathbf{distributeRWW}}([\mathbf{P_D}, \mathbf{Q_E}])$$

The distribution of recycled wastewater can be desribed using the same equations as the *Distribute Water* function (Equations 33 to 37) replacing $\mathbf{Q_F}$, $\mathbf{P_F}$, $\mathbf{Q_J}$, $\mathbf{P_J}$, $\mathbf{V}_{\mathcal{P}}$, $\mathbf{I}_{\mathcal{P}}$, and $\mathbf{Q_{Jl}}$ with $\mathbf{Q_D}^{rec}$, $\mathbf{P_D}$, $\mathbf{Q_E}$, $\mathbf{P_E}$, $\mathbf{V_N}$, $\mathbf{I_N}$ and $\mathbf{Q_{El}}$ respectively.

D. Summary of Wastewater Management System Equations

Writing the model functions defined in Sections V-A, V-B and V-C in matrix form we have a combined model for the wastewater system functions identified in Figure 17:

$$\begin{aligned}
\mathbf{Q_D} &= \mathfrak{f}_{\mathbf{collectWW}}(\mathbf{Q_J}) \\
\mathbf{I_D} &= \mathfrak{f}_{\mathbf{treatWW_I}}([\mathbf{Q_D}, \mathbf{Q_F}, \mathbf{Q_D}^{rec}]) \\
\mathbf{Q_D}^{disp} &= \mathfrak{f}_{\mathbf{treatWW_Q}}([\mathbf{Q_D}, \mathbf{Q_F}, \mathbf{Q_D}^{rec}]) \\
[\mathbf{Q_D}^{rec}, \mathbf{P_E}, \mathbf{I_N}, \mathbf{Q_{El}}] &= \mathfrak{f}_{\mathbf{distributeRWW}}([\mathbf{P_D}, \mathbf{Q_E}])
\end{aligned} \tag{43}$$

For the particular case of the models developed in each of the preceeding subsections, Equation 43 can be instantiated by combining the equations in Sections V-A, V-B and V-C providing the following system of equations:

$$\begin{bmatrix} \boldsymbol{\beta_E}(\mathbf{P_E}) & 0 & \mathbb{1}_{\mathbf{E}} & 0 \\ 0 & 0 & \mathbb{1}_{\mathbf{E}} & \mathbf{B_E}^{\dagger} \\ \mathbf{B_E} & 0 & 0 & -\mathbf{R_N}(\mathbf{Q_N}) \\ 0 & \mathbb{1}_{\mathbf{N}} & 0 & -\mathbf{K_N}\boldsymbol{\Psi_N}(\mathbf{Q_N}) \end{bmatrix} \begin{bmatrix} \mathbf{P_E} \\ \mathbf{I_N} \\ \mathbf{Q_{E_l}} \\ \mathbf{Q_N} \end{bmatrix} + \begin{bmatrix} 0 \\ \mathbf{Q_E} \\ \mathbf{B_D P_D} \\ 0 \end{bmatrix} = \begin{bmatrix} 0 \\ 0 \\ 0 \\ 0 \end{bmatrix} \tag{44}$$

$$\begin{aligned}
\mathbf{Q_D}^{rec} &= \mathbf{B_D}^{\dagger}\mathbf{Q_N} \\
\mathbf{Q_D} &= \mathbf{C_{DJ}}\mathbf{Q_J} \\
\mathbf{I_D} &= \mathbf{K_D}\mathbf{Q_D} \\
\mathbf{Q_D}^{disp} &= \mathbf{Q_D} - \mathbf{C_{DF}}\mathbf{Q_F} - \mathbf{Q_D}^{rec}
\end{aligned}$$

where $\mathbf{B_D}$, $\mathbf{B_E}$, $\mathbf{K_N}$ and $\boldsymbol{\Psi_N}$ are the equivalents of $\mathbf{B_F}$, $\mathbf{B_J}$, $\mathbf{K}_{\mathcal{P}}$ and $\boldsymbol{\Psi}_{\mathcal{P}}$ in Section IV-E.

VI. Model Outputs of Interest

Once the quantitative engineering systems model has been developed, its independent and dependent variables may be used to extract model outputs of interest. Referring back to Figure 1 the quantities A through T are given by the energy and matter flows modelled in Sections III, IV and V (Table I) .

TABLE I
ENERGY-WATER NEXUS MODEL – OUTPUTS OF INTEREST

Identifier	Formulation	Identifier	Formulation
A	$\mathbb{1}_{\mathbf{G}}\mathbf{Q_G}^{in}$	K	$\mathbb{1}_{\mathbf{F}}\mathbf{Q_F}$
B	$\mathbb{1}_{\mathbf{G}}\dot{\mathbf{M}}_{\mathbf{G}}$	L	$\mathbb{1}_{\mathbf{J}}\mathbf{Q_{Jl}} + \mathbb{1}_{\mathbf{E}}\mathbf{Q_{El}}$
C	$\mathbf{V}_{\mathcal{P}}^{\dagger}\mathbf{I}_{\mathcal{P}} + \mathbf{V}_{\mathbf{F}}^{\dagger}\mathbf{I_F}$	M	$\mathbb{1}_{\mathbf{F}}\mathbf{Q_F}^{brine}$
D	$\dot{\mathbf{m}}_{\mathbf{G}}^{\dagger}\mathbf{C_{GF}}\Delta\mathbf{H_F}$	N	$\mathbb{1}_{\mathbf{D}}\mathbf{C_{DF}}\mathbf{Q_F}$
E	$\mathbf{V}_{\mathbf{L}}^{\dagger}\mathbf{I}_{\mathbf{L_0}}$	P	$\mathbb{1}_{\mathbf{J}}\mathbf{Q_J}$
F	$\mathbf{V}_{\mathbf{G}}^{\dagger}\mathbf{I_G} - (C + E + J)$	Q	$\mathbb{1}_{\mathbf{D}}\mathbf{Q_D}$
G	$\dot{\mathbf{M}}_{\mathbf{G}}^{\dagger}\mathcal{H}_{\mathbf{G}}^{flue}$	R	$\mathbb{1}_{\mathbf{D}}\mathbf{Q_D}^{disp}$
H	$\mathbb{1}_{\mathbf{G}}\mathbf{Q_G}^{evap}$	S	$\mathbb{1}_{\mathbf{S}}\mathbf{Q_S}^{evap}$
I	$\mathbb{1}_{\mathbf{G}}\mathbf{Q_G}^{out}$	T	$\mathbb{1}_{\mathbf{E}}\mathbf{Q_E}$
J	$\mathbf{V}_{\mathbf{D}}^{\dagger}\mathbf{I_D}$		

VII. Illustrative Example

In this section, the developed model is applied to an illustrative example inspired by Egypt. The three-fold purpose of the example is to 1.) demonstrate the practical feasibility of the model, 2.) discuss its advantages over existing work 3.) discuss how it may be practically applied by an industrial practitioner. Figure 18 presents a conceptual illustration of a geographical region served by a number of different water and power sources. A complete description of the hypothetical system is described in Section VII-A. Then, the models developed in Sections III, IV, V are used to solve for measures of interest described in Section VI. These results are summarized and discussed in Section VII-B. Section VII-C concludes with a brief discussion of potential industrial application.

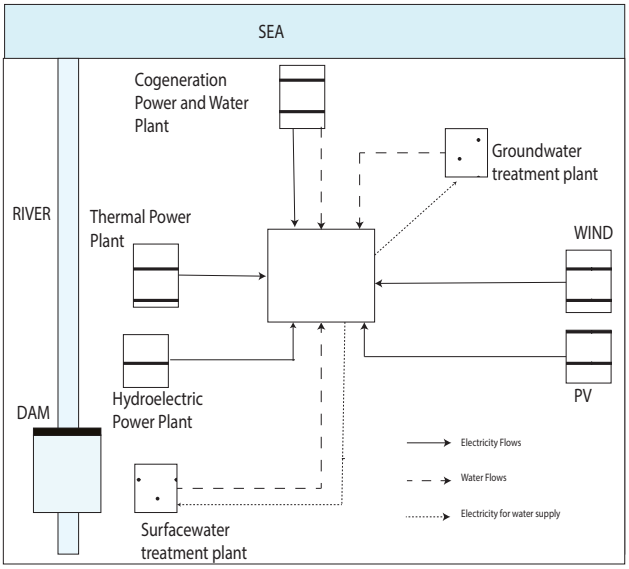

Fig. 18. Illustration inspired by Egypt

A. System Description & Model Parameters

The water distribution system is modelled as consisting of three water sources, as indicated, which are equidistant from an aggregated demand node of $6m^3/s$ or approximately 140 million gallons a day. The required hydraulic pressure for the distribution is provided entirely by pumping to the clearwell at the treatment plants. In other words, there are no additional pumps in the distribution network. A pressure equivalent to $100m$ head is assumed for all the plants. The resistance-coefficients of the three pipes serving the demand node ($\mathbf{R}_{\mathcal{P}}$ in Equation 39) are determined using the Hazen-Williams formulation assuming a pipe diameter of $2m$, a C-factor of 100 and a length of $500km$. The leakage model parameters α_j and β_j in Equation 33 are taken as 0.5 and 0.001 respectively.

The electricity distribution network for this example is modelled with the standard IEEE14 bus system [50] with the following modifications:

1) The 40MW generator at bus 2 is replaced with a 100MW generator representing a hydroelectric power plant
2) The synchrononous compensators at buses 3,6 and 8 are replaced with 10MW generators representing a solar PV plant, a wind power power plant and a thermal power plant respectively. The generator at slack bus 1 is taken as a cogeneration power plant.
3) The groundwater treatment plant, and surface water treatment plant are attached to the network at buses 5 and 14

Functions $\mathfrak{f}_{s_4}$ and $\mathfrak{f}_{h_3}$ in Equation 8 were regressed with quartic polynomials using data from ASME superheated steam and saturated water tables over the pressure range 5 to 50 bar with the specific enthalpies in MJ/kg and the specific entropies in $kJ/(kg \cdot K)$:

$$\begin{aligned} s_4 = &- 15.7881 - 0.1049p_4 + 19.3438h_4 + 0.0039p_4^2 \\ &- 6.1322h_4^2 - 0.0001p_4^3 + 0.9316h_4^3 - 0.0547h_4^4 \end{aligned} \tag{45}$$

$$\begin{aligned} h_3 = &- 61.3940 + 0.0841p_3 + 33.4630s_3 - 0.0032p_3^2 \\ &- 6.7618s_3^2 + 0.0001p_3^3 + 0.6129s_3^3 - 0.0206s_3^4 \end{aligned} \tag{46}$$

These model parameters and others necessary for the complete example are provided in Table II.

The model was implemented in the General Algebraic Modelling System (GAMS) [34] and solved with the built-in CONOPT solver [35]. No special computational facilities were required.

B. Results

The goal of this work was to develop a transparent physics-based model of the energy-water nexus model capable calculating the flows of matter and energy across and between the system boundaries of the engineered electricity,

TABLE II
MODEL PARAMETERS

Parameter	Equation	Units	Value
k_2/k_1	2	m^3/As	0.072
p_1	4	Pa	2×10^6
h_1	3, 4, 11	MJ/kg	0.909
ν_1	3, 4	m^3/kg	0.001
$\dot{\mathfrak{m}}_g$	10 - 12	kg/s	70
$\hbar_g$	12	MJ/kg	26
$\hbar_g^{flue}$	12	MJ/kg	0.8
ρ_w	11	kg/m^3	1000
c_w	11	$kJ/(kg \cdot K)$	4.1813
Δt_w	11	K	10
k_1/k_2	3, 10	$A \cdot s/m^3$	100
k_4/D	6, 10	Vs/m^3 or $J/(A \cdot m^3)$	1000
k_2/k_1	21	$A \cdot s/m^3$	100
Z	23	$(kJ/kg)/(m^3/s)$	720
RR	24	-	35 %
$q_s^{evap} \forall s$	32	m^3/s	5
$q_j \forall j$	39	m^3/s	6
$\alpha_j \forall j$	39	-	0.5
$\beta_j \forall j$	39	$(m^3/s)/Pa$	0.001
$p_f \forall f$	39	Pa	9.8×10^5
$r_p \forall p$	39	$Pa/(m^3/s)$	1057

TABLE III
RESULTS

Quantity	Value	Quantity	Value
A	$81m^3s^{-1}$	K	$9.4m^3s^{-1}$
B	$11.9kgs^{-1}$	L	$0.9m^3s^{-1}$
C	$8.5MWe$	M	$2.437m^3s^{-1}$
D	$116MWth$	N	$0m^3s^{-1}$
E	$254.2MWe$	P	$6m^3s^{-1}$
F	$8MWe$	Q	$6m^3s^{-1}$
G	$9.5MWth$	R	$6m^3s^{-1}$
H	$0m^3s^{-1}$	S	$5m^3s^{-1}$
I	$81m^3s^{-1}$	T	$0m^3s^{-1}$
J	$0MWe$		

water, and wastewater systems. To this effect, this illustrative example calculates the values of $A - T$ in Figure 1 and summarizes the results in Table III. Electricity system evaporative losses H are zero because only hydroelectric and once-through cooling plants have been modelled in this work. The wastewater system has not been modelled in this simple example and thus it can be assumed that $R = Q = P = 6m^3s^{-1}$ and that $N = 0m^3s^{-1}$.

The strength of the developed energy-water nexus becomes apparent when considering the various ratios of values $A - T$ as aggregate measures of interest. While the existing literature provides empirical evaluations of the electricity-intensity of water technologies and water-intensity of electricity technologies [13]–[18], this model calculates these results *a priori* over a larger system boundary. Consider, for example, the following ratios:

- A measure of the degree of coupling between the electricity and water systems given by $(C + J) / (C + E + F + J) = 3.2\%$
- Water supply required to sustain the electricity and water supply systems given by $A + K = 91m^3/s$
- Ratio of water displaced from its original source to total water withdrawn for water and electricity systems given by $(L + H)/(A + K) = 1.1\%$
- Proportion of water withdrawn that is returned with significantly altered quality (a measure of environmental impact) given by $(M + R)/(A + K) = 9.3\%$

In a detailed analysis, the values of each these high-level aggregate measures can be functionally traced back to

each of the power variables associated with the functions connected to values $A-T$. Thus, a change in exogenous variables like water and electricity demand growth will have subsequent and predictable changes in the water intensity of energy technologies and the energy intensity of water technologies. Furthermore, the resulting flows across the system boundary such as leaked water, brine rejection, disposable effluent, thermal and electrical and energy losses can all be calculated. In contrast, the empirically-based studies found in the literature would assume that the water and energy intensity values were constant irrespective of measurement or operating conditions. Similarly, the flows across the system boundary would be based upon these measurement assumptions. Additional measurements would have to be conducted to provide values other than just water and energy intensities. The model also well addresses changes to endogenous variables. These include the *prevalence*, *arrangement*, and *type* of water and energy technologies. For example, the model can resolve the effect of a change in the penetration level, and placement of a new (potentially undeployed) renewable energy technology. In contrast, an empirical approach assumes existing technology and does not consider the effects of technology placement. The developed model can be utilized to conduct such detailed analyses for large changes to the structure of an energy-water nexus in a particular region. Alternatively, a sensitivity analysis approach based upon the jacobian of the energy-water nexus' system of equation has already been reported [51].

C. Opportunities for Industrial Application

The advantages of a transparent physics-based energy-water nexus model described in the previous subsection can lead to a number of practical industrial applications. At the smallest scale, the merits of competing water and energy technologies can be objectively assessed not just on cost, or their individual impacts but also their impacts within the energy-water nexus as a system. A governmental regulator can use this information in permitting of various types of facilities as it evaluates the net environmental impact. On a much larger scale and over a longer time horizon, governments can apply such a model to make planning decisions across the three networks. The derived aggregate measures can be assigned an economic value to conduct integrated energy-water planning studies. Finally, because the model is physics-based it can be operationalized by integrated energy-water utilities as is commonly found in the Gulf Cooperation Council countries. Such utilities can thus monitor energy and water intensities in real-time and perhaps make energy and water dispatching decisions accordingly. In regions with separate energy and water utilities, such a model can be used to highlight areas of potential cooperation. Further discussion of such opportunities for industrial application have been reported in [52], [53].

VIII. Conclusion

This work has presented an integrated engineering systems model for the electricity, water and wastewater systems based on a previously presented reference architecture and developed with the aid of bond graphs. The model provides a set of algebraic equations that relate electricity and water demands to: (i) the requisite system inputs and concomitant system outputs for a system boundary encompassing all three grids, and (ii) the salient exchanges of matter and energy between the three systems. This modeling approach allows the definition and determination of aggregate system measures that can inform integrated planning processes. As an illustration, the presented model equations have been implemented in GAMS and used to determine a set of such aggregate measures for a hypothetical geographical region.

Future work can apply the approach and models to both planning and operations applications. The *first-pass* models used here can be enhanced to the level of detail required for different applications; critically however, in any such model refinements, the inputs and outputs of the individual functions identified in Figures 3, 12 and 17 remain the same.

References

[1] W. N. Lubega and A. M. Farid, "A Reference System Architecture for the Energy-Water Nexus," *IEEE Systems Journal*, vol. PP, no. 99, pp. 1–11, 2014. [Online]. Available: 10.1109/JSYST.2014.2302031

[2] ——, "A Meta-System Architecture for the Energy-Water Nexus," in *8th Annual IEEE Systems of Systems Conference*, Maui, Hawaii, USA, 2013, pp. 76–81. [Online]. Available: http://dx.doi.org/10.1109/SYSoSE.2013.6575246

[3] A. M. Farid and W. N. Lubega, "Powering and Watering Agriculture : Application of Energy-Water Nexus Planning," in *GHTC 2013: IEEE Global Humanitarian Technology Conference*, Silicon Valley, CA, USA, 2013, pp. 1–6.

[4] W. Lubega and A. M. Farid, "An engineering systems model for the quantitative analysis of the energy-water nexus," in *Complex Systems Design & Management*, Paris, France, 2013, pp. 219–231.

[5] R. Pate, M. Hightower, C. Cameron, and W. Einfeld, "Overview of Energy-Water Interdependencies and the Emerging Energy Demands on Water Resources," Albuquerque, New Mexico, Tech. Rep., 2007.

[6] United Nations, "Managing Water under Uncertainty and Risk," Tech. Rep., 2012.

[7] G. Olsson, *Water and Energy: Threats and Opportunities*. London: IWA Publishing, 2012.

[8] US DoE, "Energy Demands on Water Resources," Tech. Rep., 2006.

[9] World Economic Forum, "Energy Vision Update 2009 Thirsty Energy: Water and Energy in the 21st Century," Geneva, Switzerland, Tech. Rep., 2009.

[10] A. Siddiqi and L. D. Anadon, "The water energy nexus in Middle East and North Africa," *Energy Policy*, vol. 39, no. 8, pp. 4529–4540, Aug. 2011.

[11] A. S. Stillwell, C. W. King, M. E. Webber, I. J. Duncan, and A. Hardberger, "The Energy-Water Nexus in Texas," *Ecology And Society*, vol. 16, no. 1, p. 2, 2011.

[12] L. Park and K. Croyle, "California's Water-Energy Nexus : Pathways to Implementation," GEI Consultants, Inc, Tech. Rep., 2012.

[13] R. Goldstein and W. Smith, "Water & Sustainability (Volume 4): U.S. Electricity Consumption for Water Supply & Treatment - The Next Half Century," Electric Power Research Institute, Palo Alto, CA, USA, Tech. Rep. Volume 4, 2002.

[14] J. Barcel, E. Codina, J. Casas, J. L. Ferrer, and D. Garca, "A Review of Operational Water Consumption and Withdrawal Factors for Electricity Generating Technologies," Golden, CO, Tech. Rep. NREL/TP-6A20-5090, 2011.

[15] R. Goldstein and W. Smith, "Water & Sustainability (Volume 3): U.S. Water Consumption for Power Production - The Next Half Century," Electric Power Research Institute, Palo Alto, CA, USA, Tech. Rep. Volume 3, 2002.

[16] J. Macknick, R. Newmark, G. Heath, and K. C. Hallett, "Operational water consumption and withdrawal factors for electricity generating technologies: a review of existing literature," *Environmental Research Letters*, vol. 7, no. 4, p. 045802, Dec. 2012. [Online]. Available: http://stacks.iop.org/1748-9326/7/i=4/a=045802?key=crossref.6f4ebd5836ab24141e19d95fd1e65709

[17] J. Meldrum, S. Nettles-Anderson, G. Heath, and J. Macknick, "Life cycle water use for electricity generation: a review and harmonization of literature estimates," *Environmental Research Letters*, vol. 8, no. 1, p. 015031, Mar. 2013. [Online]. Available: http://stacks.iop.org/1748-9326/8/i=1/a=015031?key=crossref.d6703318287e321cce2c6d55b9a8ab76

[18] K. Averyt, J. Macknick, J. Rogers, N. Madden, J. Fisher, J. Meldrum, and R. Newmark, "Water use for electricity in the United States: an analysis of reported and calculated water use information for 2008," *Environmental Research Letters*, vol. 8, no. 1, p. 015001, Mar. 2013. [Online]. Available: http://stacks.iop.org/1748-9326/8/i=1/a=015001?key=crossref.071108cb996cfa8a02f228101d846f86

[19] A. Delgado, "Water Footprint of Electric Power Generation : Modeling its use and analyzing options for a water-scarce future," Master's thesis, 2012.

[20] M. J. Rutberg, "Modeling Water Use at Thermoelectric Power Plants," Master's thesis, Massachussets Institute of Technology, 2012.

[21] A. Santhosh, A. M. Farid, and K. Youcef-Toumi, "Real-Time Economic Dispatch for the Supply Side of the Energy-Water Nexus," *Applied Energy*, vol. 122, no. 1, pp. 42–52, 2014. [Online]. Available: http://dx.doi.org/10.1016/j.apenergy.2014.01.062

[22] A. Santhosh, A. M. Farid, A. Adegbege, and K. Youcef-Toumi, "Simultaneous Co-optimization for the Economic Dispatch of Power and Water Networks," in *The 9th IET International Conference on Advances in Power System Control Operation and Management*, 2012, pp. 1–6.

[23] A. Santhosh, A. M. Farid, and K. Youcef-Toumi, "The Impact of Storage Facility Capacity and Ramping Capabilities on the Supply Side of the Energy-Water Nexus," *Energy*, vol. 66, no. 1, pp. 1–10, 2014. [Online]. Available: http://dx.doi.org.libproxy.mit.edu/10.1016/j.energy.2014.01.031

[24] ——, "The Impact of Storage Facilities on the Simultaneous Economic Dispatch of Power and Water Networks Limited by Ramping Rates," in *IEEE International Conference on Industrial Technology*, Cape Town, South Africa, 2013, pp. 1–6.

[25] A. Santhosh, A. M. Farid, and K. Youcef-toumi, "Optimal Network Flow for the Supply Side of the Energy-Water Nexus," in *2013 IEEE International Workshop on Intelligent Energy Systems*, Vienna, Austria, 2013, pp. 1–6.

[26] W. N. Lubega, A. Santhosh, A. M. Farid, and K. Youcef-Toumi, "An Integrated Energy and Water Market for the Supply Side of the Energy-Water Nexus in the Engineered Infrastructure," in *ASME 2014 Power Conference*, Baltimore, MD, 2014, pp. 1–11.

[27] ——, "Unit Commitment for a Supply Side Market of the Energy-Water Nexus," *submitted to: IEEE Transactions on Sustainable Energy*, vol. 1, no. 1, pp. 1–8, 2014.

[28] V. C. Tidwell, P. H. Kobos, L. Malczynski, G. Klise, W. E. Hart, and C. Castillo, "Decision Support for Integrated Water- Energy Planning," SANDIA National Lab, Tech. Rep. October, 2009.

[29] S. Sattler, J. Macknick, D. Yates, F. Flores-Lopez, A. Lopez, and J. Rogers, "Linking electricity and water models to assess electricity choices at water-relevant scales," *Environmental Research Letters*, vol. 7, no. 4, p. 045804, Dec. 2012. [Online]. Available: http://stacks.iop.org/1748-9326/7/i=4/a=045804?key=crossref.e1597dc96fe929476c24435da0dce544

[30] S. Friedenthal, A. Moore, and R. Steiner, *A Practical Guide to SysML: Systems Modeling Language*. San Francisco, CA, USA: Morgan Kaufmann Publishers Inc., 2008.

[31] M. Otter, H. Elmqvist, and F. E. Cellier, "Modeling of multibody systems with the object-oriented modeling language Dymola," *Nonlinear Dynamics*, vol. 9, no. 1-2, pp. 91–112, Feb. 1996.

[32] J. Akesson, K.-E. Arzen, M. Gaafvert, T. Bergdahl, and H. Tummescheit, "Modeling and optimization with Optimica and JModelica.org—Languages and tools for solving large-scale dynamic optimization problems," *Computers & Chemical Engineering*, vol. 34, no. 11, pp. 1737–1749, Nov. 2010. [Online]. Available: http://www.sciencedirect.com/science/article/pii/S009813540900283X

[33] J. Frenkel, C. Schubert, G. Kunze, P. Fritzson, M. Sjölund, and A. Pop, "Towards a benchmark suite for Modelica compilers: Large models," in *Modelica'2011: The 8th International Modelica Conference*, 2011.

[34] R. Rosenthal and R. E.Rosenthal, "GAMS Users Guide," Washington, Tech. Rep., 2012. [Online]. Available: http://www.gams.com/dd/docs/bigdocs/GAMSUsersGuide.pdf

[35] A. Drud, "Conopt," ARKI Consulting and Development A/S, Bagsvaerd, Denmark, Tech. Rep., 2013. [Online]. Available: http://www.gams.com/dd/docs/solvers/conopt.pdf

[36] D. Karnopp, D. L. Margolis, and R. C. Rosenberg, *System dynamics : a unified approach*, 2nd ed. New York: Wiley, 1990.
[37] F. T. Brown, *Engineering System Dynamics*, 2nd ed. Taylor & Francis, 2007.
[38] G. Gonzalez and O. Barriga, "A Hydroelectric Plant connected to an Electric Power System," in *Recent Advances in Technologies*, M. Strangio, Ed. Intech Open Access Publisher, 2009, ch. 11, pp. 181–198. [Online]. Available: http://www.intechopen.com/books/recent-advances-in-technologies/
[39] P. Kiameh, *Power generation handbook : fundamentals of low-emission, high-efficiency power plant operation*, 2nd ed. New York: McGraw-Hill, 2012.
[40] A. Leva and C. Maffezzoni, "Modelling of power plants," in *Thermal Power Plant Simulation and Control*, D. Flynn, Ed., London, 2003, ch. 2, pp. 17–57.
[41] T. Bakka and H. Karimi, "Wind turbine modeling using the bond graph," in *IEEE International Symposium on Computer-Aided Control System Design*, 2011, pp. 1208–1213.
[42] A. Cipollina, G. Micale, and L. Rizzuti, *Seawater desalination : conventional and renewable energy processes*. Berlin ; London: Springer, 2009.
[43] C. Sommariva, *Desalination and Advanced Water Treatment : Economics and Financing*. Massachussetts ; USA: Balaban Desalination Publications, 2010.
[44] J. Gebel, *An Engineer's Guide to Desalination*. Vgb Powertech, 2008.
[45] O. Giustolisi, D. Savic, and Z. Kapelan, "Pressure-driven demand and leakage simulation for water distribution networks," *Journal of Hydraulic Engineering*, vol. 134, no. 5, pp. 626–635, 2008.
[46] M. Tabesh, M. Jamasb, and R. Moeini, "Calibration of water distribution hydraulic models: A comparison between pressure dependent and demand driven analyses," *Urban Water Journal*, vol. 8, no. 2, pp. 93–102, Apr. 2011. [Online]. Available: http://www.tandfonline.com/doi/abs/10.1080/1573062X.2010.548525
[47] P. J. Mosterman, "Hybrid Dynamic Systems: A Hybrid Bond Graph Modeling Paradigm and its Application in Diagnosis," Ph.D. dissertation, Vanderbilt University, 1997. [Online]. Available: http://msdl.cs.mcgill.ca/people/mosterman/papers/thesis/
[48] J. Thoma and B. O. Bouamama, *Modelling and Simulation in Thermal and Chemical Engineering*. Germany: Springer Verlag, 2010.
[49] G. Tchobanoglous, F. L. Burton, and D. H. Stensel, *Wastewater Engineering: Treatment and Reuse*, 4th ed. New York, N.Y.: McGraw Hill, 2004.
[50] F. Milano, *Power System Modelling and Scripting*. Springer Verlag, 2010.
[51] W. N. Lubega and A. M. Farid, "An Engineering Systems Sensitivity Analysis Model for Holistic Energy-Water Nexus Planning," in *ASME 2014 Power Conference*, Baltimore, MD, 2014, pp. 1–10.
[52] W. N. Lubega, A. Santhosh, A. M. Farid, and K. Youcef-Toumi, "Opportunities for Integrated Energy and Water Management in the GCC – A Keynote Paper," in *EU-GCC Renewable Energy Policy Experts' Workshop*, no. December, Masdar Institute, Abu Dhabi, UAE, 2013, pp. 1–33. [Online]. Available: http://www.grc.net/data/contents/uploads/Opportunities_for_Integrated_Energy_and_Water_Management_in_the_GCC_5874.pdf
[53] W. N. Lubega and A. M. Farid, "Opportunities for Integrated Energy-Water Nexus Management in the Gulf Cooperation," *submitted to: Energy Policy*, pp. 1–11, 2014.